



# High-resolution flexible tactile sensors

Zicheng Shen<sup>#</sup>, Hui Wu<sup>#</sup>, Yuyu Hou, Geng Yang, Huayong Yang<sup>\*</sup> , Kaichen Xu<sup>\*</sup> 

## Keywords:

Tactile sensors, high spatial resolution, flexible sensors, artificial intelligence

**Citation:** Shen, Z.; Wu, H.; Hou, Y.; Yang, G.; Yang, H.; Xu, K. High-resolution flexible tactile sensors. *Soft Sci.* 2026, 6, 53. <https://dx.doi.org/10.20517/ss.2026.77>

**Received:** 15 Apr 2026

**First Decision:** 13 May 2026

**Revised:** 20 May 2026

**Accepted:** 1 Jun 2026

**Published:** 18 Jun 2026

## Academic Editor:

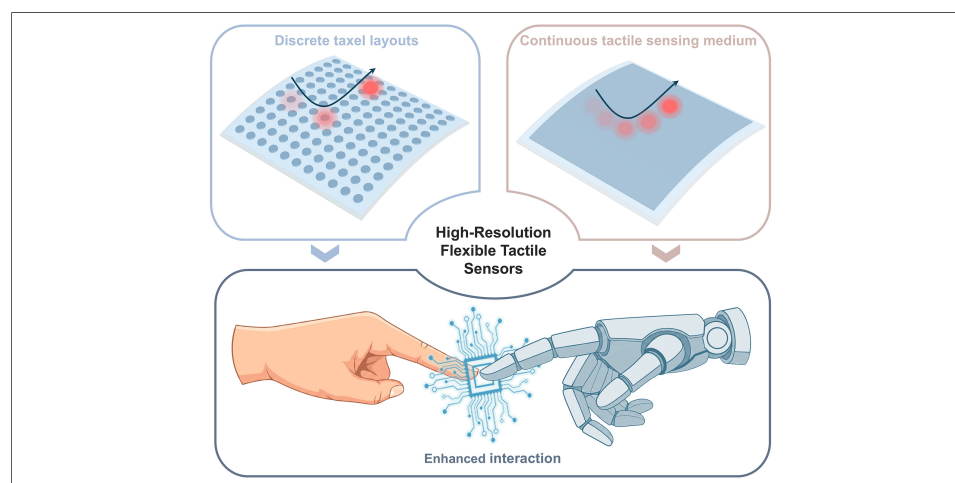
Nae-Eung Lee

## Copy Editor:

Pei-Yun Wang

## Production Editor:

Pei-Yun Wang



## Abstract

Flexible tactile sensors serve as the essential sensory interfaces for compliant physical interaction in advanced intelligent systems, such as embodied intelligence robotics and smart wearable devices. To meet the increasing demand for rich and precise tactile information, achieving high-resolution perception has become a vital performance metric for these flexible tactile sensing systems. This review presents a systematic overview of flexible tactile sensors from the perspective of high-resolution realization mechanisms, mainly encompassing two paradigms: array-based spatial information sampling via discrete taxel layouts, and array-free spatial information inference over continuous tactile sensing medium. First, dense taxel layouts are introduced as conventional array-based strategies for high-resolution realization. Then, the emerging sparse layout strategies enabled by artificial intelligence (AI) algorithms are described, achieving super-resolution sensing beyond physical layout density. Subsequently, we summarize the array-free strategies for high-resolution tactile sensing over continuous sensing medium, focusing on physics-based inference and learning-based prediction. In addition, we show typical examples of their applications in enhanced interaction scenarios. Finally, future trends toward scalable, generalizable, multimodal, and highly integrated flexible tactile sensing systems are discussed, with scientific challenges and potential development pathways outlined.



State Key Laboratory of Fluid Power and Mechatronic Systems, School of Mechanical Engineering, Zhejiang University, Hangzhou 310058, Zhejiang, China.

<sup>#</sup>Authors contributed equally.

**\*Correspondence to:** Prof. Huayong Yang, Prof. Kaichen Xu, State Key Laboratory of Fluid Power and Mechatronic Systems, School of Mechanical Engineering, Zhejiang University, Hangzhou 310058, Zhejiang, China. E-mail: yhy@zju.edu.cn; xukc@zju.edu.cn

## INTRODUCTION

Tactile sensing, unlike vision or audition, represents a fundamental and direct modality for interacting with the physical world<sup>[1,2]</sup>. In biological systems, human skin serves as a typical paradigm of this capability. It functions as a highly intricate sensory network and continuously acquires a wealth of physical information, such as contact state, surface texture, and temperature. Such rich tactile information enables humans to effortlessly perceive the outside environment and perform delicate manipulations<sup>[3,4]</sup>. Inspired by this exquisite biological mechanism, diverse tactile sensors are designed to emulate these sensory capabilities. By transducing mechanical stimuli at the contact interface into interpretable signals, tactile sensors enable artificial systems to perceive physical contact events in a well-defined manner. This capability provides an essential sensory foundation for advanced intelligent systems [e.g., dexterous robotics, embodied artificial intelligence (AI), and smart wearable devices], whose performance increasingly depends on accurate and real-time tactile feedback<sup>[5-8]</sup>.

Despite this critical demand, traditional tactile sensors, typically fabricated on rigid substrates like silicon, metals, or ceramics, suffer from a fundamental mechanical mismatch with soft biological tissues and complex curved surfaces. Their intrinsic rigidity hinders conformal integration, leading to unreliable signal acquisition and degraded performance during dynamic interactions on deformable substrates. In contrast, flexible sensing technologies have addressed these limitations through innovative material or structure designs<sup>[9-12]</sup> and novel fabrication paradigms<sup>[13-16]</sup>. Relying on advanced flexible manufacturing and heterogeneous integration technologies, various functional sensitive units can be assembled onto different flexible substrates. These engineered flexible sensors can precisely measure a wide range of physical parameters, including normal pressure<sup>[17-19]</sup>, surface strain<sup>[20,21]</sup>, shear force<sup>[22]</sup>, vibration<sup>[23]</sup>, and temperature<sup>[24]</sup>. At the same time, their flexible architectures endow them with attractive mechanical properties, such as ultrathin profile, tunable mechanical modulus, excellent bendability, and significant stretchability. Benefiting from these attributes, flexible tactile sensors exhibit intrinsic compliance and can seamlessly adhere to curvilinear robotic skeletons or soft human skin, thereby mitigating the mechanical mismatch and ensuring more robust acquisition of high-quality tactile signals<sup>[25]</sup>.

However, as intelligent systems are deployed in increasingly complex scenarios, the requirements for flexible tactile sensing are rapidly extending beyond simple contact detection toward finer spatial perception. Tactile sensing with higher spatial resolution enables robotic systems to perceive surface texture details, edge contours, and local geometric variations of objects. By complementing these fine contact information with visual perception, it allows robotic systems to better understand their surroundings and perform more adaptive exploration in unstructured environments<sup>[26]</sup>. Human-machine interaction tasks likewise require higher level tactile perception, as more refined tactile information helps systems more accurately interpret contact information, thereby improving the effectiveness and responsiveness of physical interaction<sup>[27]</sup>. In addition, many physiological signals manifested on the human body surface are accompanied by localized pressure changes and subtle deformations, such as pulse-induced pressure fluctuations and respiration-related deformation<sup>[28]</sup>. Access to finer-grained tactile sensing can improve the accuracy and reliability of physiological signal acquisition in health monitoring devices<sup>[29]</sup>. As a result, the demands placed on flexible tactile sensors are steadily evolving toward more precise perception and richer representation of spatial details, making high-resolution sensing a key performance target for further advances in the field. In this context, high resolution primarily refers to high spatial resolution, namely the capability of a tactile system to resolve and localize spatially distributed contact stimuli within a defined sensing region. However, it should be noted that the evaluation of spatial resolution is inherently dependent on the underlying realization paradigm of the tactile systems. Different flexible tactile sensing architectures adopt distinct mechanisms for acquiring and interpreting spatial information, and therefore their criteria used to quantify high spatial resolution are not universally identical.

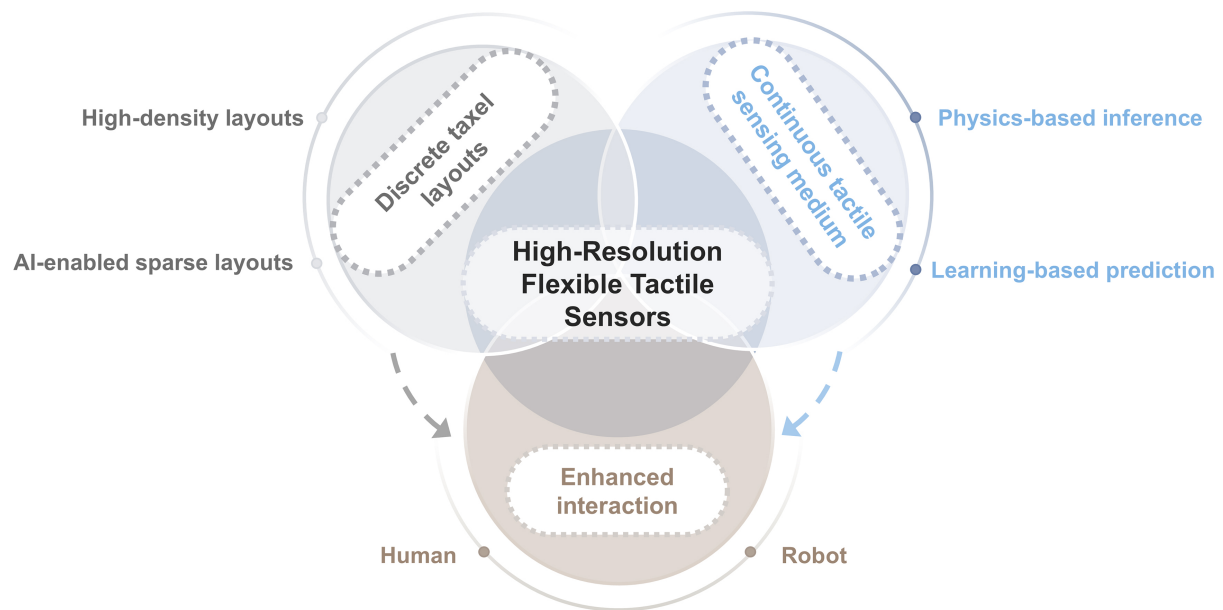


**Figure 1.** Overview of realization paradigms and target applications for high-resolution flexible tactile sensors. AI: Artificial intelligence.

Considering these paradigm-dependent differences, a unified perspective is needed to understand how high-resolution flexible tactile sensing is realized across different architectures. Existing reviews have extensively discussed flexible tactile sensors from the viewpoints of material designs, transduction mechanisms, device structures, and application scenarios<sup>[30–32]</sup>. However, a systematic understanding of flexible tactile sensors from the perspective of high-resolution realization mechanisms remains limited, particularly with regard to how spatial information is acquired, inferred, and evaluated in fundamentally different sensing architectures. Clarifying these realization mechanisms can help reveal the underlying design logic of high-resolution flexible tactile sensors and provide guidance for matching sensing architectures with specific application requirements. From this perspective, this review categorizes high-resolution flexible tactile sensing into two major realization paradigms: array-based spatial information sampling via discrete taxel layouts, and array-free spatial information inference over continuous tactile sensing medium. In the first paradigm, tactile information is acquired through localized sampling by spatially distributed sensing units (taxels), and the achievable spatial resolution remains largely tied to the spatial layout of these predefined sampling sites<sup>[33–35]</sup>. In the second paradigm, a continuous sensing medium interacts with distributed contact stimuli and generates integrated physical responses, which are collected electrically or optically by a limited number of terminal devices<sup>[36–38]</sup>. Spatial tactile information is then inferred from these global responses through computational decoding. The essential distinction between these two paradigms therefore lies in how spatial tactile information is obtained: one through discrete local sampling at predefined taxel locations, and the other through computational inference from global readout signals of a continuous sensing field.

As shown in [Figure 1](#), in the following sections, this review systematically maps the recent progress in high-resolution flexible tactile sensors through the lens of these two fundamental realization paradigms. We begin by dissecting array-based strategies that enhance spatial resolution through structured dense taxel layouts and AI algorithms-assisted sparse layout designs. Then, the focus shifts to array-free architectures based on the continuous sensing medium, highlighting both physics-informed inference and learning-based prediction frameworks. Representative applications are subsequently discussed to illustrate how high-resolution flexible tactile sensors empowers advanced interactions in both human-centric and robot-driven scenarios. Finally, we summarize prevailing challenges and outline open opportunities for future developments of high-resolution flexible tactile systems.

## HIGH-RESOLUTION TACTILE SENSING ENABLED BY SPATIAL LAYOUTS OF TAXELS

A taxel represents the fundamental sensing unit in array-based tactile systems. Each taxel independently transduces mechanical stimuli (e.g., normal pressure, shear force, or strain) into measurable electrical signals through various physical mechanisms, including piezoresistive<sup>[39]</sup>, capacitive<sup>[40]</sup>, piezoelectric<sup>[41]</sup>, or triboelectric<sup>[42]</sup> effects. At the level of an individual unit, a taxel primarily provides localized amplitude information that reflects the stimulus magnitude around its immediate vicinity. To acquire spatially distributed tactile information over the interested region, multiple taxels are arranged into spatial layouts, thereby forming a tactile sensor array. The realization of such flexible tactile arrays commonly relies on several representative process routes: printing-based methods, laser processing, three-dimensional forming techniques, and lithographic fabrication. Printing-based methods, such as screen printing, inkjet printing, aerosol printing, and direct ink writing, are typically used to deposit conductive electrodes, sensing materials, and interconnect patterns on flexible substrates in a cost-effective and scalable manner. Laser processing, including laser scribing, laser ablation, and laser-induced functionalization, offers a mask-free and digitally programmable route for defining sensing pixels, conductive traces, and local isolation structures. Three-dimensional forming techniques, such as fused deposition modeling, photocuring-based 3D printing, and 3D-printing-assisted molding or curing, are particularly useful for constructing microstructured surfaces, elastic supporting layers, and conformal three-dimensional device geometries. In addition, lithographic fabrication, often combined with thin-film deposition and etching, provides high patterning precision and is therefore especially important for dense miniaturized arrays and transistor-based backplanes. These process routes differ in attainable feature size, processing efficiency, material compatibility, and integration capability, which are usually selected according to the intended array architecture and sensing mechanism. For more detailed discussions of specific fabrication workflows and process optimization, readers are referred to dedicated reviews on flexible sensor manufacturing<sup>[43-45]</sup>.

After achieving a taxel array, the spatial tactile map can be obtained by aggregating signals from taxels distributed over different locations. From this perspective, array-based tactile sensing can be interpreted as a spatial sampling process, analogous to pixelated imaging systems. The output of each taxel is intrinsically linked to a fixed spatial coordinate, indicating that positional information is directly embedded in the signal. Thus, spatial resolution is typically defined by structural parameters such as taxel pitch and layout density. Improving spatial resolution in such systems naturally implies increasing the effective sampling density.

### Dense taxel layouts for high-resolution

Driven by the demand for finer tactile perception in advanced intelligent systems, researchers have progressively pursued denser taxel layouts as a straightforward means of improving spatial resolution. Through shrinking taxel dimensions and reducing taxel pitch, taxel arrays can achieve higher layout density to approximate continuous spatial sampling within a defined sensing region. In practice, such dense taxel arrays can be broadly divided into two architectural forms based on their readout methods: passive-matrix and active-matrix configurations.

Passive-matrix taxel arrays represent a conventional yet widely adopted solution for dense spatial sampling. In this architecture, taxels are placed at the intersection of shared electrode lines in a row–column configuration, where row lines and column lines are selected sequentially to complete a scan of the whole tactile map<sup>[46,47]</sup>. This scheme effectively reduces wiring complexity compared to individually wired taxels and thus appears naturally scalable toward high-density layouts<sup>[48]</sup>. However, as taxel size decreases and array density increases, passive-matrix taxel arrays become increasingly constrained by crosstalk, which fundamentally limits their effective spatial resolution<sup>[49]</sup>. Crosstalk in dense passive arrays arises from coupled electrical and mechanical effects, but these two effects degrade the actual sensing resolution through different pathways. Electrically, the absence of local switching elements permits unintended current paths and

parasitic coupling through shared lines under matrix addressing. As electrode spacing decreases, those effects in the shared network become more pronounced, leading to signal leakage and spurious responses in neighboring taxels<sup>[50]</sup>. Consequently, ghost responses or false activations may appear in the final tactile map readout even when no real mechanical stimulus is applied at those taxel locations. Mechanically, localized deformation in flexible substrates can spread laterally through compliant layers and interconnect structures. When taxels are densely packed, a single load may therefore induce simultaneous deformation in neighboring units, leading to blurred tactile maps and increasing the minimum distinguishable distance beyond the nominal taxel pitch<sup>[51]</sup>. Therefore, electrical crosstalk primarily introduces readout-level spatial ambiguity, whereas mechanical crosstalk broadens the physical stimulus response at the material and structural levels. Both mechanisms explain why reducing taxel pitch alone does not necessarily ensure improved spatial fidelity or actual sensing resolution.

To mitigate these issues, several system-level strategies have been explored. For electrical crosstalk, one common route is circuit-level optimization of matrix readout. Representative methods include voltage-feedback schemes<sup>[52]</sup> and zero-potential schemes<sup>[53]</sup>. Algorithm-assisted correction methods have also been used to compensate for readout errors without relying entirely on hardware design<sup>[54]</sup>. In addition, electrical shielding or insulating structures can be introduced to suppress parasitic coupling and unintended current spreading in dense taxel grids. For mechanically induced crosstalk, decoupling designs are often adopted to confine local deformation. Typical examples include modulus regulation<sup>[55]</sup>, bridge structures<sup>[56]</sup>, and mechanical isolation features such as grooves or other supporting structures<sup>[57]</sup>. These approaches collectively seek to preserve spatial separability while maintaining high taxel density, thus enabling high resolution tactile perception capability.

**Figure 2A** shows a crosstalk-free high-resolution pressure sensor array fabricated via a two-step laser manufacturing strategy. In this design, low-power laser-induced graphitization locally converts polyimide into conductive porous graphene to define electrically isolated sensing units, while a subsequent high-power laser cutting step forms serpentine interconnects that mechanically decouple adjacent units. By combining taxel-level electrical isolation with strain-dissipating structural design, the device effectively suppresses both electrical and mechanical crosstalk. As a result, the array achieves a spatial resolution of 0.7 mm with significantly reduced interference (crosstalk coefficient down to -43.63 dB)<sup>[58]</sup>. **Figure 2B** presents a high-density strain sensor array that achieves unprecedented spatial resolution through the Fowler-Nordheim (F-N) tunneling effect of monodispersed spiky carbon nanospheres (SCNs). The authors construct a dense, matrix-addressable array by assembling a highly ordered SCN film and precisely defining the sensing units via laser scribing. Subsequently, silver/polydimethylsiloxane (PDMS) composite interconnects are printed alongside pure PDMS insulators, which are strategically dispensed at the intersections of the longitude and latitude lines to prevent electrical short circuits. By seamlessly co-curing these elastomeric components into a unified sensing film, the device realizes a remarkable sensing density of 100 pixels cm<sup>-2</sup> and exceptional inter-unit consistency (standard deviation  $\leq 3.82\%$ ) for high-fidelity strain field mapping<sup>[59]</sup>.

In contrast to passive matrices, active-matrix arrays incorporate switching elements at each sensing node, most commonly transistors or diodes, enabling electrically isolated addressing<sup>[60,61]</sup>. In these transistor-based implementations, the gate is typically connected to the row-select line (word line) and the drain is connected to the column-readout line (bit line), while source is in series with the tactile sensing element or ground<sup>[62]</sup>. Mechanical stimuli modulate either the impedance of sensing elements or the intrinsic gate potential and channel conductivity of the transistor itself. Consequently, this modulation alters the output drain current under an applied bias<sup>[63]</sup>. Because each taxel is addressed through a gated conduction channel rather than direct current flow through shared lines, selective activation can be achieved at the node level. During

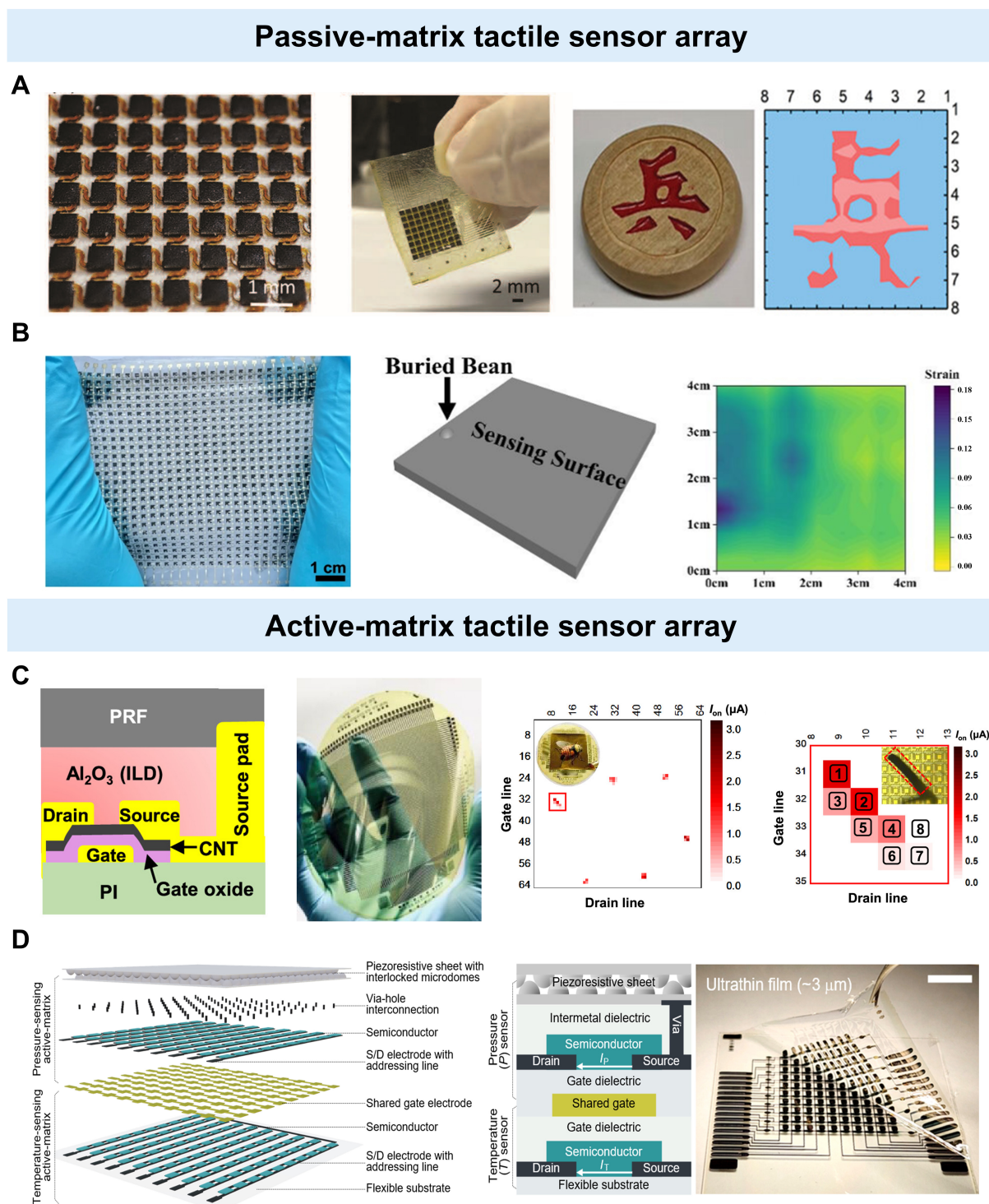


**Figure 2.** High-density taxel arrays for high-resolution tactile sensing implemented in passive-matrix and active-matrix architectures. (A) A passive-matrix flexible pressure sensor array with serpentine interconnects, enabling high spatial resolution and suppressed crosstalk. Reproduced with permission from Ref.<sup>[58]</sup>, Copyright © 2022 Wiley; (B) A high-density strain sensing array based on self-assembled and patterned SCNs for detailed strain field mapping. Reproduced from Ref.<sup>[59]</sup> under the CC BY 4.0 license, Copyright © 2024 The Author(s); (C) Large-scale integrated flexible pressure sensor array with CNT TFT active matrix, achieving enhanced spatial resolution and minimizing crosstalk. Reproduced with permission from Ref.<sup>[66]</sup>, Copyright © 2022 American Chemical Society; (D) 3D active-matrix multimodal sensor array with vertically stacked TFT-based pressure and temperature sensors, which enable independent spatial mapping of pressure and temperature. Reproduced from Ref.<sup>[67]</sup> under the CC BY-NC license, Copyright © 2025 The American Association for the Advancement of Science. SCNs: Spiky carbon nanospheres; CNT: carbon nanotube; TFT: thin-film transistor; PRF: piezoresistive film; ILD: interlayer dielectric; PI: polyimide.

readout, only the transistors in the activated row are turned on by the gate-select signal, allowing the corresponding taxels to be connected to the column readout lines. In contrast, the transistors in non-selected rows remain in the off state and present a high impedance between the sensing elements and the readout path. As a result, non-selected taxels cannot form effective sneak-current paths through the shared matrix network, which substantially suppresses signal leakage during sequential addressing. This node-level switching mechanism significantly reduces electrical crosstalk in dense arrays. Among active-matrix architectures, thin-film transistor (TFT)-based arrays are particularly attractive for high-resolution flexible tactile systems due to their compatibility with planar microfabrication processes<sup>[64]</sup>. Using lithographic patterning, vapor deposition, or solution-based thin-film techniques, large-scale functional device arrays can be monolithically fabricated in a compact footprint<sup>[65]</sup>. This enables thousands of independently addressable taxels to be arranged with reduced readout interference.

Figure 2C presents a large-area active-matrix tactile sensor array that integrates a piezoresistive film with carbon nanotube (CNT) TFTs to achieve high-density, electrically isolated readout. In this work, each sensing unit is coupled to a CNT-TFT that functions as a local switching element. The pressure-sensitive film modulates the electrical signal at the source node, and the gated conduction channel ensures that only the selected taxels contribute to the readout current, effectively suppressing crosstalk during sequential scanning. The demonstrated  $64 \times 64$  array, featuring a remarkable taxel pitch of 0.9 mm, achieves stable pressure mapping over a large area (e.g., resolving the footprint of an artificial honeybee)<sup>[66]</sup>. Advancing beyond unimodal detection, Figure 2D demonstrates a 3D transistor-on-transistor active-matrix architecture designed for the independent, spatially resolved sensing of both pressure and temperature. Each pixel features a vertical stack: a top one-transistor-one-resistor (1T-1R) pressure sensor, comprising a TFT coupled to a large-area reduced graphene oxide/polyvinylidene difluoride (rGO/PVDF) interlocked microdome piezoresistive sheet, is situated directly above a bottom 1T temperature sensor. Both layers cleverly share a common gate line to streamline matrix readout. To resolve the temperature cross-sensitivity of TFT-based pressure readouts, the authors introduce a calibrated compensation strategy. They use the co-located temperature signal to correct thermally distorted pressure currents, successfully reducing temperature-induced variability in pressure readout by ~99%. The demonstrated  $10 \times 10$  3D active-matrix array (scale bar 1 cm) achieves accurate and high-resolution 2D mapping of pressure over 0-20 kPa and temperature over 25-50 °C<sup>[67]</sup>.

However, it is crucial to recognize that while active switching effectively suppresses electrical crosstalk, mechanical coupling between neighboring taxels remains a fundamental bottleneck for spatial resolution. Furthermore, integrating thin-film switching elements introduces inherent trade-offs, including heightened fabrication complexity, increased power consumption, and long-term reliability challenges under repeated mechanical deformation<sup>[68]</sup>. Therefore, while active matrices provide a structurally robust solution for high-density addressing, further improvements in effective spatial resolution still depend on coordinated system-level optimization. In summary, scaling down taxel pitch represents the most intuitive strategy for achieving high-resolution tactile sensing. Both passive and active matrices rely on this geometric densification to approximate continuous spatial perception through discrete sensing nodes. However, the preceding analysis underscores that true spatial resolution is not exclusively dictated by physical miniaturization. As array density scales, electrical crosstalk, mechanical coupling, fabrication complexity, interconnect scalability, and power constraints collectively impose practical limits. Consequently, continuously shrinking taxel size becomes increasingly costly and inefficient as a means of improving effective resolution. To circumvent these physical hardware limitations, recent research has begun to leverage computational methods to enhance the effective resolution of spatial tactile sensing. By pairing sparse taxel layouts with advanced signal processing and AI algorithms, this approach offers a highly promising route to achieving high-resolution perception with reduced hardware complexity.

### AI-assisted super-resolution tactile sensing

Unlike dense artificial taxel arrays that pursue higher spatial resolution primarily through geometric miniaturization, the human skin naturally achieves remarkable tactile acuity despite a relatively sparse distribution of mechanoreceptors. Biological tactile perception relies on a continuous, mechanically coupled skin layer beneath which specialized receptors are distributed at discrete locations<sup>[69]</sup>. Mechanical stimuli applied at the surface propagate through the compliant tissue, forming distributed strain and pressure fields that are sampled by those underlying receptors. Through the integration of signals from multiple receptors and higher-level neural processing, the human somatosensory system is capable of resolving spatial features finer than the average receptor spacing - a phenomenon often described as tactile hyperacuity or biological super-resolution (SR)<sup>[70]</sup>. This biological architecture suggests that high spatial resolution does not necessarily require an absolutely one-to-one correspondence between sensing units and spatial sampling density. Instead, it may stem from the joint decoding of related signals triggered by a single contact. Inspired by this principle, recent research in flexible tactile sensors has begun to explore architectures wherein sparse taxel arrays are embedded within compliant flexible substrates<sup>[71,72]</sup>. In these designs, the mechanical coupling effect of the elastomer serves a critical transducing function: localized external mechanical stimuli induce regional strain diffusion, simultaneously activating multiple adjacent discrete taxels. Consequently, individual sensing units are no longer restricted to strict and independent point-to-point mapping. They exhibit overlapping receptive fields and spatial correlations, highly analogous to the biological somatosensory system. With access to these spatially correlated multi-channel signals and the known positional priors of the taxel layout, traditional interpolation computational methods can complement the missing information between predefined sampling sites, thereby recovering spatial details in a certain extent<sup>[73]</sup>.

The rapid development of AI and data-driven algorithms further enables this paradigm shift. By leveraging machine learning models capable of extracting high-dimensional features from correlated taxel responses, it becomes possible to reconstruct high-resolution tactile maps precisely from a limited number of sensing units<sup>[74,75]</sup>. Within this framework, sparse taxel layouts combined with AI algorithms aim to achieve SR tactile sensing like human skin, where the effective spatial resolving capability exceeds the geometric spacing of taxels. The evaluation of such SR capability generally follows two complementary perspectives. From a structural viewpoint, one may quantify how many distinguishable virtual contact points can be resolved between adjacent physical taxels, reflecting the SR factor achieved relative to the number and spacing of real sensing units<sup>[76]</sup>. This perspective characterizes how effectively sparse measurements are converted into finer virtual spatial sampling. From a performance-oriented viewpoint, SR is directly quantified by localization accuracy, typically measured through statistical error metrics such as root mean square error (RMSE) or mean absolute error (MAE)<sup>[77,78]</sup>. These metrics reflect how precisely the inferred contact position or pressure distribution matches the ground truth. Together, these two evaluation strategies provide a comprehensive understanding of whether a sparse tactile system genuinely surpasses its geometric sampling limits. In the following sections, we define SR factor as dividing taxel spacing by the localization prediction error (RMSE or MAE) to quantify the SR capability.

**Figure 3A** presents a magnetosensitive electronic-skin (e-skin) that achieves SR tactile localization through sparse magnetic sensing units combined with computational decoding methods. The device consists of a flexible magnetic film with a one-dimensional sinusoidal magnetization profile and a sparse array of Hall sensors positioned underneath. When external forces deform the flexible magnetic layer, the resulting continuous 3D magnetic flux variations can be smoothly modulated and sampled by the underlying sensor array. Owing to the spatial continuity of the magnetic field, each sensing unit captures overlapping and correlated magnetic responses. Leveraging a machine learning algorithm to decode these distributed magnetic variations, the system successfully achieves a localization MAE of 0.1 mm with a physical spacing of 6 mm between neighboring Hall sensors, yielding a remarkable SR factor of 60<sup>[79]</sup>. **Figure 3B** demonstrates

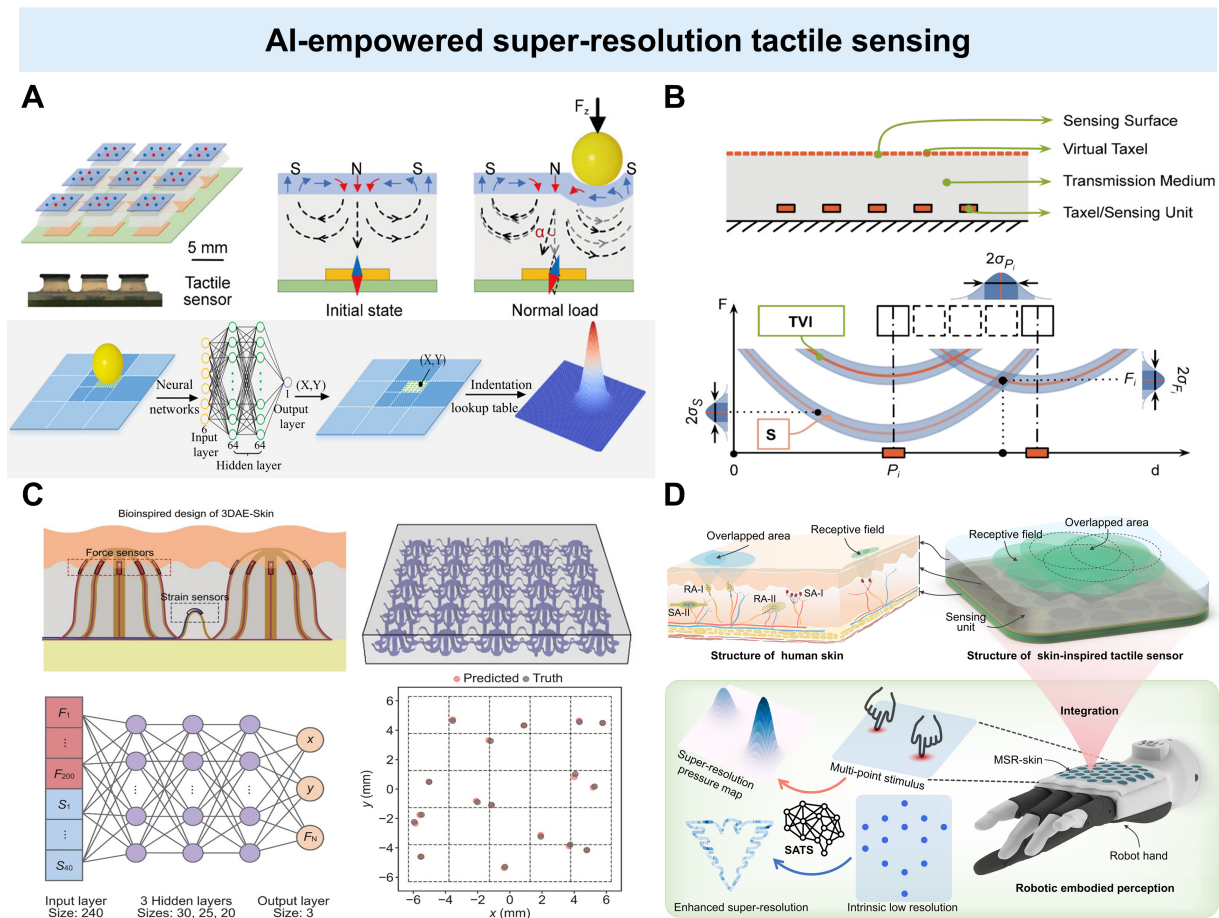


**Figure 3.** SR tactile sensing enabled by AI algorithms with sparse taxel layouts. (A) Soft magnetic e-skin that combines a sparse Hall-sensor array with a sinusoidally magnetized flexible film, enabling force self-decoupling and deep learning-enhanced tactile SR. Reproduced with permission from Ref.<sup>[79]</sup>, Copyright © 2021 The American Association for the Advancement of Science; (B) A barometer-based tactile skin with a sparse array embedded in an elastomer for SR contact localization. Reproduced with permission from Ref.<sup>[80]</sup>, Copyright © 2022 The American Association for the Advancement of Science; (C) Tactile e-skin with a bioinspired 3D layout of force and strain sensors, enabling SR sensing through decoupled multimodal mechanosensation. Reproduced with permission from Ref.<sup>[81]</sup>, Copyright © 2024 The American Association for the Advancement of Science; (D) A skin-inspired sparse taxel array with overlapped receptive fields, where a self-attention-assisted deep learning model reconstructs SR pressure distributions. Reproduced from Ref.<sup>[82]</sup> under the CC BY 4.0 license, Copyright © 2025 The American Association for the Advancement of Science. SR: Super-resolution; AI: artificial intelligence; e-skin: electronic-skin; TVI: taxel value isoline; 3DAE-Skin: three-dimensionally architected electronic skin; RA: rapid adapting; SA: slowly adapting; SATS: self-attention-assisted tactile super-resolution; MSR: multi-point super-resolution.

a geometric SR tactile skin that embeds a sparse 5-by-5 grid of barometric units, within a continuous elastomeric transmission medium. This architecture relies on the elastic properties of the material, which lead to a characteristic spread of contact information to the underlying sensing taxels. External contact forces deform the transmission medium, allowing the barometers to sense local volume changes in the form of isotropic pressure. To solve the inverse problem of inferring high-resolution tactile information from these sparse measurements, the system employs a data-driven multilayer perceptron (MLP) neural network. This signal processing approach successfully localizes the contact position with an average RMSE of 0.161 mm. With 6.5 mm physical taxel spacing, this system achieves a SR factor of 40, effectively creating highly resolved virtual taxels from a limited number of physical sensors<sup>[80]</sup>. Figure 3C highlights a three-dimensionally architected electronic skin (3DAE-Skin) that biomimetically mirrors the spatial distribution of Merkel cells and Ruffini endings in human skin. The device features spatially distributed arrays of force and strain sensors encased in a heterogeneous elastomeric encapsulation. With a physical spacing of 2.5 mm between sensing units, the vertical separation structures intrinsically isolate mechanical

stimuli, enabling the fully decoupled perception of normal forces, shear forces, and tensile strains. By using a deep neural network (DNN) to decode the spatially correlated piezoresistive responses, the system achieves SR contact localization with a RMSE of just 0.117 mm, corresponding to a SR factor of approximately 21<sup>[81]</sup>. **Figure 3D** reports SR tactile sensor arrays with sparsely distributed taxels enabled by a universal intelligent framework. The authors combine a topology-optimized taxel layout, which is designed to maximize overlapped receptive-field coverage, with a self-attention-assisted tactile super-resolution (SATS) model. By aggregating correlated tactile information across the overlapping receptive fields, the SATS model successfully reconstructs a dense 54 × 50 SR pressure map. This remarkable extrapolation generates 2,700 high-fidelity virtual taxels from just 23 physical nodes, resulting in a spatial upsampling factor of ~117<sup>[82]</sup>. Furthermore, the system exhibits an average localization RMSE of 0.73 mm, approaching human fingertip-level acuity. Crucially, the framework leverages zero-shot generalization to robustly reconstruct complex multi-point pressure distributions by training solely on single-point data. By evaluating the 0.73 mm localization precision against the array's physical taxel pitch of 10.5 mm, the system finally achieves a SR factor of 14.4.

### HIGH-RESOLUTION TACTILE SENSING INDEPENDENT OF TAXEL LAYOUTS

As discussed above, array-based flexible tactile sensing systems have achieved substantial progress in high-resolution perception through both dense taxel layouts and sparse arrays assisted by computational enhancement. Nevertheless, their spatial information acquisition remains fundamentally anchored to predefined taxel locations. As effective resolution continues to improve or sensing scale expands further, such systems are typically accompanied by a growing number of sensing units and more complex interconnects, along with heavier readout burdens. These inherent structural limitations have motivated the exploration of alternative realization strategies for high-resolution tactile perception.

Departing from spatially discrete sampling in array-based tactile systems, the second realization paradigm employs a continuous functional medium as the sensing layer (e.g., a piezoresistive/piezocapacitive film or an optical layer). External contact alters the regional electrical, mechanical, or optical state of this continuous medium, and the resulting state variations are collected by a limited number of terminal devices, such as distributed electrodes, optical cameras, or other readout ports<sup>[83-85]</sup>. Instead of corresponding to predefined local sampling sites, each readout channel reflects an integrated response of the continuous medium under a given measurement configuration, for example, voltages measured across different electrode pairs or optical images captured from a specific viewpoint. Then, the spatial tactile information can be inferred from these global responses by computational decoding methods. As a result, the effective spatial resolution becomes more dictated by the analytical precision and decoding capacity of the applied inference framework. On this basis, array-free tactile sensing architectures can be broadly categorized into two realization mechanisms. The first relies on physics-based inference. In this class of methods, the relationship between physical state changes in the continuous medium and the global responses is explicitly described by a forward physical model governed by known mathematical equations, as exemplified by conductivity perturbation models in electrical impedance tomography (EIT)<sup>[86]</sup> and field-distribution models in capacitive sensing media<sup>[87]</sup>. Spatial tactile information can be recovered by inverting this forward model, typically through regularized optimization or finite-element-based simulations. Thus, due to its distinctive reliance on interpretable physical priors, the achievable spatial resolution in practice is mostly defined by the consistency between the assumed forward physical model and the real sensing system.

**Figure 4A** reports an interconnect-free, array-free tactile mapping interface that achieves high-resolution perception via EIT. The device features an ultrathin (~50 μm), intrinsically stretchable continuous sensing medium composed of a homogeneous piezoresistive nanocomposite (multiwall CNTs embedded in an elastomer matrix). The system solves the EIT inverse problem by utilizing global voltage measurements

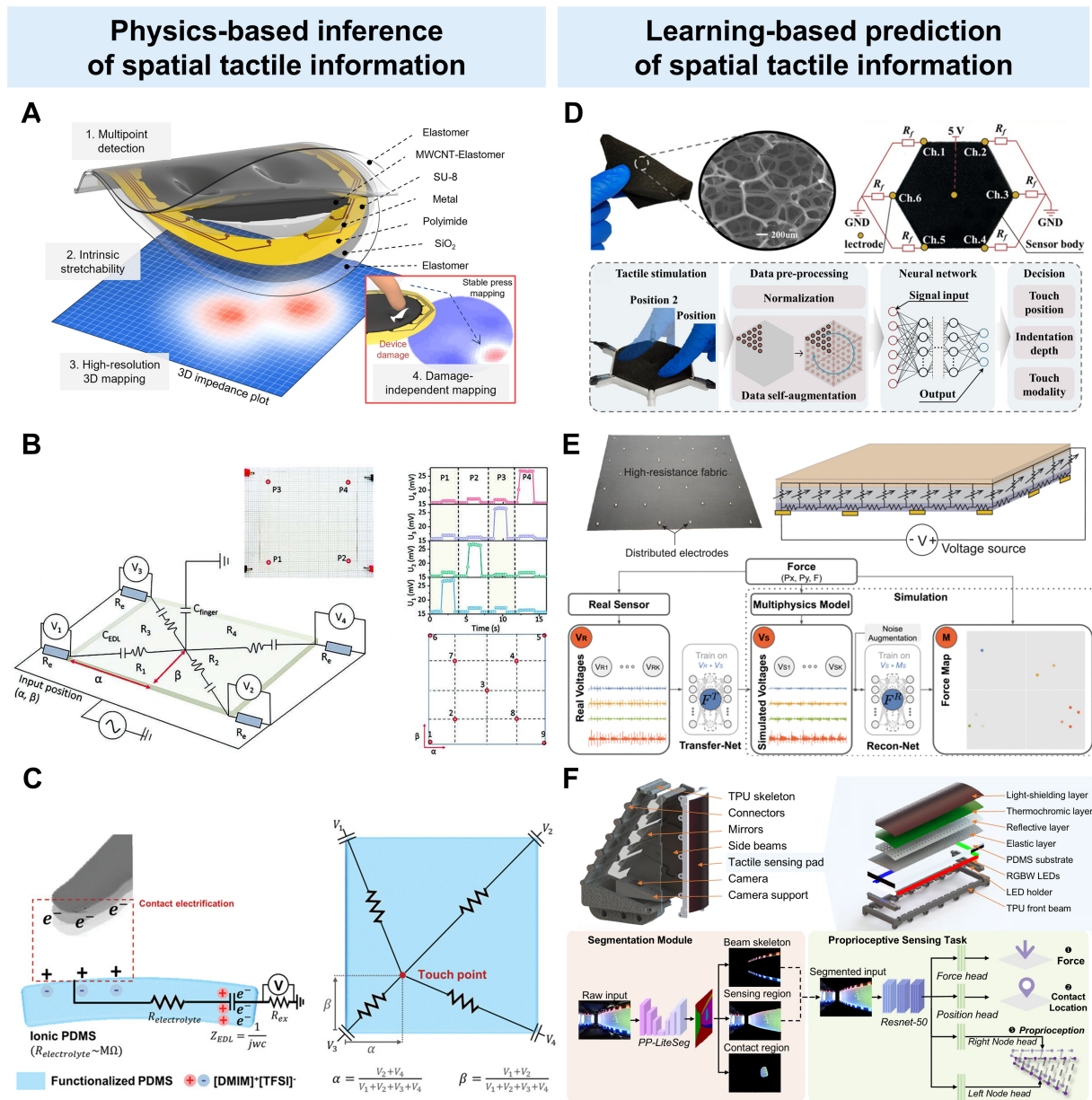


**Figure 4.** Physics-based inference and learning-based prediction of spatial tactile information in array-free tactile sensing architectures. (A) An ultrathin EIT-based soft e-skin for high-resolution tactile mapping with multipoint detection and damage tolerance operation. Reproduced from Ref.<sup>[88]</sup> under the CC BY-NC license, Copyright © 2024 The American Association for the Advancement of Science; (B) SFITS that determines touch positions on a continuous ionic film from distributed voltage signals. Reproduced with permission from Ref.<sup>[89]</sup>, Copyright © 2025 Wiley; (C) Grid-free triboresistive touch sensor based on monolayered ionic PDMS for touch-point recognition. Reproduced with permission from Ref.<sup>[90]</sup>, Copyright © 2022 Wiley; (D) Bioinspired hexagonal tactile sensor combined with deep learning for spatially continuous touch localization and modality recognition. Reproduced from Ref.<sup>[95]</sup> under the CC BY 4.0 license, Copyright © 2022 The Author(s); (E) A hybrid sim-to-real learning framework for force-map reconstruction in a large-area ERT-based tactile sensor. Reproduced from Ref.<sup>[96]</sup> under the CC BY-NC-ND 4.0 license, Copyright © 2022 The Author(s); (F) A compliant visuotactile gripper with a multi-mirror optical system and a decoupled deep learning framework for accurate multimodal haptic perception under large deformation. Reproduced from Ref.<sup>[97]</sup> under the CC BY-NC-ND license, Copyright © 2025 The Author(s). EIT: Electrical impedance tomography; e-skin: electronic-skin; SFITS: silk fibroin ionic touch screen; PDMS: polydimethylsiloxane; ERT: electrical resistance tomography; MWCNT: multiwall carbon nanotube; GND: ground; TPU: thermoplastic polyurethane; RGBW: red, green, blue, white; LEDs: light emitting diodes.

collected from merely 16 peripheral electrodes, algorithmically inverting the pressure-induced conductivity perturbations to a  $40 \times 40$  virtual tactile map encompassing 920 effective pixels. This translates to a pixel-to-terminal ratio exceeding 57, thereby demonstrating exceptional virtual information density. At the

same time, the spatial fidelity of the virtual grid is rigorously validated through millimeter-scale localization tests. It can successfully decouple and distinguish multiple physical stimuli spaced at strict 1-mm intervals. In addition, by dynamically updating the reference state within the EIT algorithm, the reconstructed pressure maps remain remarkably stable even under severe irreversible damage (e.g., physical razor cuts) or temperature fluctuations, indicating the high resilience of this physics-based inverse reconstruction paradigm<sup>[88]</sup>. Figure 4B demonstrates another representative array-free tactile interface based on a continuous silk fibroin ionic conductor. In its two-dimensional configuration, the system employs only four peripheral electrodes located at the corners of the sensing medium. When a touch occurs, the contact-induced coupling capacitance perturbs the uniform electrostatic field across the continuous medium, and the precise spatial coordinates are analytically inferred from the distributed boundary voltage measurements. Rigorous spatial fidelity evaluations using a  $9 \times 9$  uniform touch grid reveal that the peripheral regions initially exhibited nonlinear spatial distortion due to inherent boundary field effects, yielding a maximum normalized positioning error of 0.216. However, by coupling physics-guided finite-element method (FEM) simulations with a radial basis function (RBF) correction algorithm, this spatial shift was computationally calibrated, successfully reducing the normalized error to below 0.06. Furthermore, the voltage–distance relationship maintains strict linearity even under 100% tensile strain and extensive cyclic loading, demonstrating highly robust field inference despite severe mechanical deformation<sup>[89]</sup>. Sharing a fundamentally similar physical inference architecture, the grid-free triboresistive touch sensing platform in Figure 4C is defined by a subtle yet crucial mechanistic distinction: a completely self-powered operation. This platform leverages a homogeneous monolayered ionic PDMS sheet where contact electrification inherently generates a local electric field. Upon touch, the localized electrostatic perturbation drives an induced current, and the system measures the redistributed voltage signals at the corners, which are inversely proportional to the internal resistance between the touch point and each terminal. By solving this physics-based field inference model, the exact touch coordinates are analytically inferred. This approach also achieves exceptional spatial fidelity, successfully distinguishing spatial inputs with a strict 1-mm resolution<sup>[90]</sup>. Similar low-electrode non-taxel strategies have also been extended from pure position acquisition to multimodality. For example, Huang *et al.* proposed a layered location-and-pressure intelligent tactile sensor composed of a top Ag conductive film, a middle CNT and porous polyurethane (PU) pressure-sensitive layer, and a bottom graphite conductive film for continuous dual-modal tactile location and pressure perception<sup>[91]</sup>. It avoids densely distributed sensing units and decodes touch information from electrical redistribution within a continuous functional structure. The graphite layer enables pixel-less position perception through current shunting, while the CNT@PU layer provides pressure-sensitive amplitude modulation, allowing synchronized decoding of touch location and pressure using only three electrodes and two public output channels. This design achieves a location precision below 0.4 mm and a pressure detection limit of 75 Pa, supporting intention-driven human-machine interaction applications.

Although the above physics-based array-free tactile systems may appear similar to commercial capacitive touch screens in terms of tactile position acquisition, their structural design goals and implementation routes are substantially different. Commercial capacitive touch screens generally detect local capacitance variations across dense arrays and are mainly optimized for planar coordinate input on rigid or slightly flexible interfaces. In contrast, the physics-based array-free tactile systems discussed here use only a few peripheral electrodes to collect global field responses from a continuous flexible medium, aiming to realize spatial tactile inference on soft, stretchable, and deformable interfaces. This transition from rigid planar touch input to flexible tactile mapping relies on both materials innovation and physical decoding architectures: flexible conductive composites, ionic gels, elastomers, and robust electrode–medium interfaces provide stable continuous sensing media, while simplified electrode configurations and physics-based inference models decode spatial contact information from limited boundary readouts. Future efforts should further improve material homogeneity, low-hysteresis response, interfacial stability, and model robustness under bending,

stretching, pressure loading, and environmental drift, thereby moving toward practical flexible touch-screen-like tactile systems.

However, when the relationship between contact stimuli and global readout signals becomes too nonlinear or highly coupled to be accurately described by explicit physical models, learning-based prediction frameworks provide another realization mechanism for array-free tactile perception. In contrast to the physical-based methods, the learning-based pathway treats the continuous sensing medium as a highly complex physical information encoder. Here, various neural networks [e.g., convolutional neural networks (CNNs) or DNNs] are employed to directly learn the mapping between global measurements and distributed spatial contact states. Rather than depending on exact forward physical modeling, these systems approximate the underlying forward–inverse relationship implicitly through data-driven optimization<sup>[92–94]</sup>. This data-driven parallel paradigm significantly broadens the designing freedom of array-free tactile sensors, enabling them to bypass the theoretical bottlenecks of analytical modeling and exhibit exceptional decoding ability when confronting highly complex medium properties or physical interactions that defy precise mathematical formulation. It should be noted that this learning-based array-free paradigm is fundamentally different from AI-assisted sparse taxel arrays in terms of the physical meaning of sensing and readout channels. In sparse taxel arrays, the system consists of multiple sensing units sparsely arranged at predefined spatial positions, and each sensing unit generally provides a local readout channel that reflects the mechanical response around its own location. Learning algorithms then infer high-resolution tactile information by enhancing, interpolating, or correlating these sparse local measurements. In contrast, an array-free tactile system can be regarded as a single continuous sensing body equipped with multiple readout terminals distributed at different positions. These terminals do not function as local taxels; instead, they collect different global responses of the same continuous medium, in which the spatial information of contact stimuli is mixed and encoded through the electrical, mechanical, or optical field of the material. Therefore, this paradigm is categorized as array-free spatial inference rather than array-based SR.

As a representative implementation of this learning-based paradigm, [Figure 4D](#) demonstrates an array-free tactile system utilizing a continuous piezoresistive medium. The sensor comprises a carbon black-coated PU sponge, where global resistance variations are extracted via a single center electrode and six peripheral boundary terminals. To process the highly complex nonlinear porous mechanics of the sponge, the system employs a customized DNN that directly maps these sparse readout signals into spatial touch states. Quantitatively, the model achieves robust spatial localization on unseen test locations, reporting MAE of  $3.83 \pm 2.88$  mm for radius and  $3.79^\circ \pm 3.47^\circ$  for angle<sup>[95]</sup>. Furthermore, to overcome the data-intensive bottleneck typical of deep learning approaches, this work ingeniously exploits the structural geometry of the hexagonal sensor. By introducing a symmetry-based self-augmentation strategy, the training dataset is computationally expanded sixfold, which drastically reduces the empirical data collection burden by up to 98.1% while fully preserving the model's spatial generalization capabilities. [Figure 4E](#) presents a hybrid sim-to-real learning framework for force-map reconstruction in a large-area electrical resistance tomography (ERT)-based tactile sensor. In this architecture, the continuous piezoresistive sensing surface is composed of conductive textile layers and a conductive foam layer, while 28 distributed electrodes collect sequential voltage measurements from the deformable sensing medium. The authors construct an electromechanical multiphysics model to synthesize voltage responses under diverse multi-contact conditions and further combine it with two DNNs. Transfer-Net first learns the discrepancy between real and simulated voltage measurements, while Recon-Net reconstructs the spatial force map from the transferred voltage signals. By leveraging approximately 290,000 simulated measurements and 90,000 real measurements, this modular pipeline improves multi-contact force-map prediction on a 540 mm × 560 mm tactile surface. In unseen real multi-contact tests, the best-performing configuration achieved an average contact localization error of 74.4 mm, a force estimation error of 17.2%, and a contact diameter prediction error of -9.3%, outperforming both purely physics-based

reconstruction and direct end-to-end learning<sup>[96]</sup>. Beyond the aforementioned electrical signal encoding schemes, this data-driven paradigm demonstrates equally profound decoding capabilities within the optical domain. Figure 4F illustrates a flexible visual-tactile sensory gripper that seamlessly integrates a highly compliant Fin Ray skeleton with a continuous multi-layered sensing pad. To monitor dynamic physical interactions, the system employs an internal multi-mirror optical arrangement, enabling a single camera to continuously capture global high-resolution images of both direct contact deformations and mirror-reflected views. As large-scale structural bending and complex multi-mirror reflections generate highly intertwined global optical signals, the system utilizes a decoupled deep learning framework to process the visual data. Customized CNNs are deployed to directly map these raw global images into five distinct haptic modalities. Specifically, the learning models achieve a fine spatial resolution of 0.96 mm for contact localization, alongside exceptional accuracies of 0.17 N for normal force and 0.24 mm for spatial proprioception. Coupled with a 1.17 °C temperature estimation accuracy, the neural network-based implicit mapping successfully translates complicated optical interferences into rich informational cues, ensuring high-fidelity, full-coverage tactile reconstruction during highly deformable physical interactions<sup>[97]</sup>.

Beyond the above two broadly discussed routes based on physical-based inference and learning-based prediction, on-site optical visualization provides another material-driven strategy for array-free tactile position acquisition. In this approach, the sensing medium itself generates local color change or light emission at the stimulated region, allowing contact position, object shape, and pressure distribution to be directly visualized without constructing a dense electrical sensor matrix. Representative mechanisms include mechanoluminescence, piezophotonics, pressure-controlled electrochromism, and structural color changes<sup>[98]</sup>. For example, an octopus-inspired hybrid device integrates ionic pressure sensing with electrochromic visualization, enabling pressure magnitude, contact position, and object shape to be perceived through both capacitance signals and visible color changes<sup>[99]</sup>. This strategy can provide intuitive spatial feedback and reduce the dependence on external data-processing or display modules.

In conclusion, despite the structural simplicity and scalability advantages of array-free tactile sensing architectures, several inherent bottlenecks continue to constrain their practical deployment and ultimate perceptual fidelity. For physics-based inference frameworks, the inference process is commonly bound to inverse problems, which are notoriously ill-posed and highly sensitive to boundary conditions<sup>[100]</sup>. Consequently, even minute measurement noise or subtle forward-model discrepancies (e.g., electrode configuration mismatches or medium inhomogeneity) may be amplified during inversion, ultimately leading to reduced spatial fidelity of the reconstructed information. This limitation becomes particularly critical in long-term robotic or wearable deployment, where material aging, repeated deformation, and environmental variations may gradually alter the actual physical response of the sensing medium and make it deviate from the assumed theoretical model, resulting in unstable performance. In addition, the adopted physical model often defines the perceptual modality of the system. For example, EIT-based reconstruction is typically more suitable for recovering quasi-static conductivity or pressure-induced perturbation distributions, whereas accurate dynamic force sensing remains challenging because the boundary voltage responses may be affected by the high coupling of normal and shear interactions. Similarly, field-based touch models can provide efficient coordinate inference under simplified contact assumptions, but their analytical formulations may become less reliable when facing multi-point contacts and complex force distributions. Conversely, while learning-based prediction models elegantly bypass physics-based inversion, they introduce a heavy reliance on dataset richness and distributional representativeness<sup>[101]</sup>. Although DNNs achieve exceptional intra-distribution accuracy, they frequently suffer severe performance degradation when confronting out-of-distribution (OOD) scenarios. In practical applications, such OOD conditions may arise from unseen contact conditions (e.g., dynamic force, variations of loading speed and contact geometry), uncalibrated environmental fluctuations, and device-to-device differences<sup>[102-105]</sup>. These factors can cause distribution shifts

between the training dataset and real operating data, making it difficult for a model trained under predefined conditions to accurately predict tactile information in continuously changing interaction scenarios. Furthermore, the “black-box” nature of purely data-driven approaches often lacks physical interpretability, undermining their reliability in safety-critical interactive applications. Moreover, from a system-level perspective, an inherent tension persists between computational complexity and real-time responsiveness. Extracting high-resolution spatial information across expansive continuous areas necessitates either solving high-dimensional inverse matrices or executing DNNs, both of which impose substantial latency and energy overheads, posing significant challenges for both high-frequency interactive and resource-constrained systems<sup>[106]</sup>.

Looking forward, the next leap in array-free high-resolution tactile sensing will likely be driven by several synergistic advancements. The integration of physics-informed machine learning (e.g., physics-informed neural networks, PINNs) promises to bridge the gap between model-based interpretability and data-driven robustness, profoundly stabilizing the reconstruction of ill-posed problems under limited measurements<sup>[107]</sup>. Incorporating adaptive calibration and self-supervised learning mechanisms will be beneficial to maintaining lifelong algorithmic reliability against inevitable material degradation and environmental drifts<sup>[108]</sup>. In conclusion, the array-free paradigm is not poised to entirely replace discrete array-based architecture. Rather, it serves as a powerful complementary pathway, shifting the mechanism of high-resolution perception from spatial sampling of discrete taxel to the algorithmic inversion of continuous sensing medium. The continued evolution of physical modeling, data-driven learning, and system integration techniques will determine how effectively this paradigm can support future intelligent interaction systems.

## APPLICATION

Whether employing dense taxel arrays, algorithmically enhanced sparse layouts, or computational inference over continuous sensing media, these high-resolution flexible tactile sensing systems share a unified objective: to effectively and precisely resolve spatially distributed contact information within a defined sensing region. Such spatially detailed tactile information significantly improves a system’s ability to interpret complex contact stimuli, playing a critical role in interaction tasks<sup>[109-111]</sup>. In practice, these advanced tactile systems primarily serve two distinct subjects. The first subject encompasses robotic systems, which integrate tactile sensing to intelligently engage with physical objects, explore unstructured environments, and accomplish complex interactive tasks<sup>[112,113]</sup>. The second subject involves human users, for whom tactile systems act as interactive platforms to connect with machines, teleoperated proxies, or extended reality (XR) environments<sup>[114-118]</sup>. In the following sections, we analyze representative interaction scenarios for both subjects and discuss how high-resolution tactile information contributes to improved interaction performance.

For robotic systems, tactile perception functions as a critical feedback channel during active physical interaction. Particularly in robot–object interaction scenarios, this high spatially resolved tactile feedback is vital for executing stable grasping, early slip detection, and dexterous manipulation<sup>[119]</sup>. [Figure 5A](#) illustrates the adaptive robotic grasping of fragile objects under external disturbances, enabled by high-resolution feedback from a SR magnetic tactile skin with sparse taxel layout. The fundamental advantage of this intelligent tactile system lies in its dual capability: driven by the SR framework, it not only achieves sub-millimeter contact localization but also extracts highly sensitive, self-decoupled normal gripping forces ( $F_z$ ) and external shear forces ( $F_x$ ) at that precise contact node. In the first case, when a grasped fragile egg is subjected to an unpredictable downward dragging force, the system continuously monitors the  $F_x/F_z$  ratio at the localized contact interface. Through evaluating this real-time grasping state against the strict boundaries of the physical friction cone, the robotic hand detects incipient sliding trends and adaptively tightens its grip to maintain a secure hold, immediately relaxing the pressure once the disturbance subsides to prevent

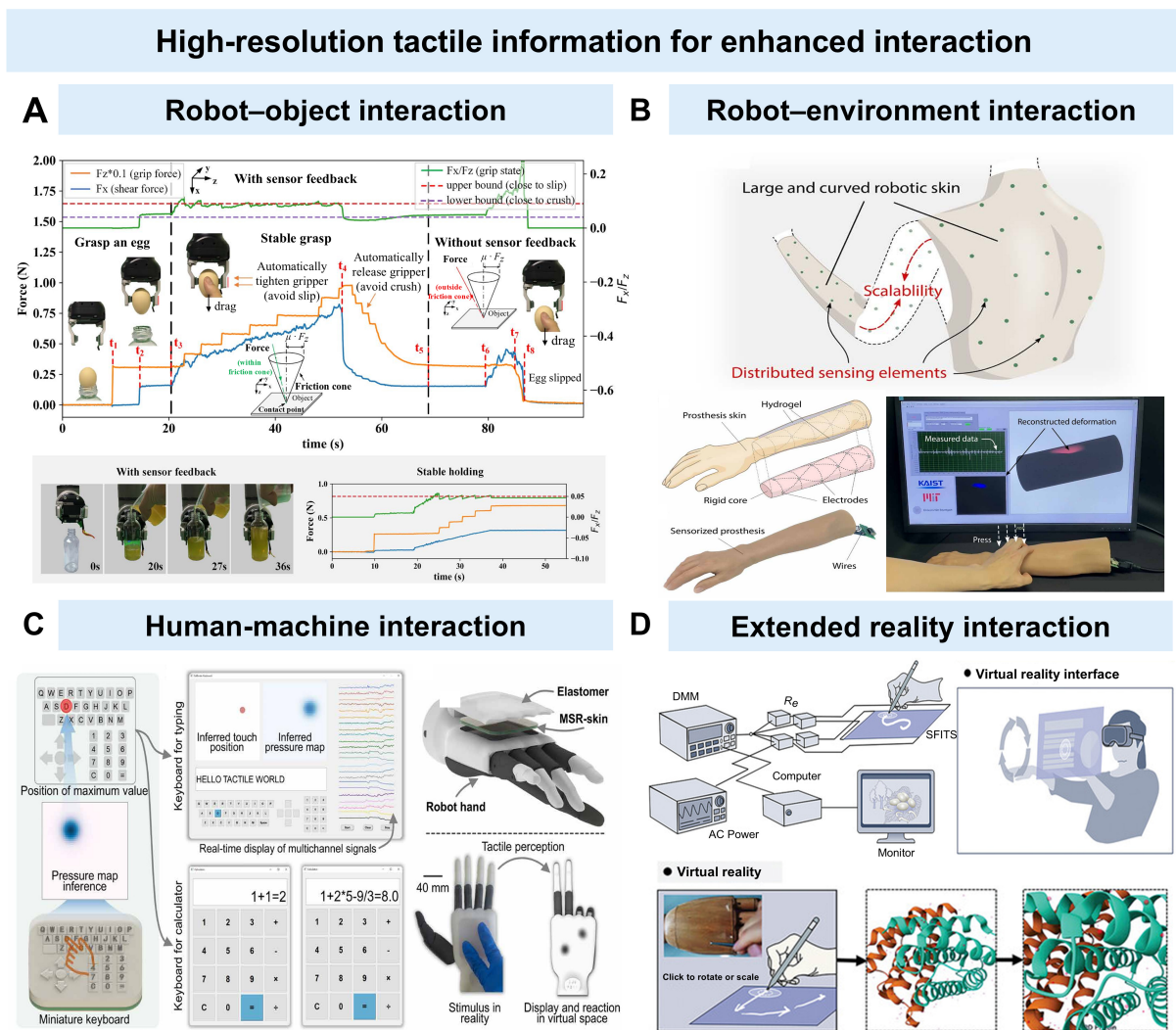


**Figure 5.** Applications of enhanced interaction enabled by high-resolution flexible tactile sensors. (A) Robot–object interaction involving stable grasping and adaptive holding enabled by a soft magnetic skin with SR localization and self-decoupled force sensing. Reproduced with permission from Ref.<sup>[79]</sup>, Copyright © 2021 The American Association for the Advancement of Science; (B) Robot–environment interaction supported by large-area tactile perception on curved prostheses using a biomimetic hydrogel-based e-skin. Reproduced with permission from Ref.<sup>[121]</sup>, Copyright © 2022 The American Association for the Advancement of Science; (C) Human–machine interaction using a SR sparse taxel array, including a miniaturized tactile keyboard and embodied tactile perception on a robot hand. Reproduced from Ref.<sup>[82]</sup> under the CC BY 4.0 license, Copyright © 2025 The American Association for the Advancement of Science; (D) XR interaction based on a SFITS that converts touch and handwriting inputs into commands for manipulating 3D virtual models. Reproduced with permission from Ref.<sup>[89]</sup>, Copyright © 2025 Wiley. SR: Super-resolution; e-skin: electronic-skin; XR: extended reality; SFITS: silk fibroin ionic touch screen; MSR: multi-point super-resolution; DMM: desktop multimeter; AC: alternating current.

crushing. Similarly, when securing a bottle continuously filled with water, the tactile feedback loop dynamically intensifies the normal gripping force to counteract the progressively increasing downward shear, actively preventing macroscopic slip. This synergy of highly precise localization and decoupled mechanics highlights a highly promising pathway for delicate manipulation in unstructured setups<sup>[79]</sup>.

Beyond localized object manipulation, high-resolution tactile sensing is equally indispensable for large-scale robot–environment interactions, where physical contacts frequently occur across expansive and curved surfaces. Unlike precision grasping, which exploits high-density tactile information within a confined footprint for localized force regulation, environmental interaction highlights the critical ability of maintaining high-fidelity spatial resolution over broad, continuous areas<sup>[120]</sup>. In these scenarios, robotic

systems must not only detect the occurrence of contact but also reconstruct high-fidelity spatial pressure distributions to facilitate precise collision localization, safe physical human-robot interaction (pHRI) and whole-body compliant control. [Figure 5B](#) presents a biomimetic hydrogel electronic skin that synergistically integrates physics-based EIT reconstruction and passive acoustic sensing to enable large-area array-free tactile perception. The system utilizes a compliant ionic hydrogel as a continuous tactile medium, strategically embedded with sparsely distributed electrodes. As demonstrated on large and curved robotic surface or custom-molded prosthetic arm, this hydrogel-based electronic skin can seamlessly conform to complex 3D geometries. Through inverse reconstruction algorithms, the device achieves accurate localization and deformation maps reconstruction of external stimuli across a broad sensing area. Such reconstruction capability enables robotic platforms to perceive environmental contact over extended surfaces, thereby supporting adaptive interaction behaviors<sup>[121]</sup>.

Beyond the above task-specific demonstrations, high-resolution tactile sensing further serves as a key perceptual foundation for embodied intelligence in robotic systems for future development. Embodied intelligence requires robots to acquire, update, and utilize physical knowledge through continuous interaction with objects and environments, rather than relying solely on visual recognition or pre-defined motion planning<sup>[122]</sup>. In this context, spatially resolved tactile feedback transforms physical contact into structured contact-state representations, including contact location, pressure distribution, force gradients, and whole-body contact maps<sup>[123]</sup>. These rich tactile representations enable robots to evaluate the consequences of their own actions and adapt subsequent motor commands, thereby supporting contact-aware manipulation, tactile-guided exploration, and interaction-driven policy learning<sup>[7,26,83]</sup>. Therefore, high-resolution tactile sensing is not merely an enhancement of local sensing accuracy, but an essential interface through which robotic agents close the perception-action loop and develop more adaptive behaviors in unstructured real-world environments.

Shifting the focus to human-centered interactive systems, high-resolution flexible tactile sensors functions as a critical interface that seamlessly translates human physical contact into precise digital interpretations<sup>[124]</sup>. In this context, the primary advantage of high spatial resolution lies in fundamentally expanding the information bandwidth of the interactive platform. By accurately capturing fine-grained, spatially distributed contact patterns within a limited interface area, the system can meticulously distinguish a vast array of subtle touch behaviors, including multi-point inputs, and complex sliding trajectories. This capability allows the tactile interface to encode an exceptionally high density of interactive commands into a compact physical footprint, avoiding the need for cumbersome mechanical buttons layout and enabling highly efficient and convenient human-digital communication.

Exemplifying this high-bandwidth encoding, [Figure 5C](#) illustrates a SR tactile skin that pairs a sparsely distributed sensor array with a self-attention-assisted deep learning framework. Leveraging this computationally enhanced resolution, a customized miniature keyboard is directly mapped onto a compact continuous sensing area. During user interaction, the reconstructed high-fidelity pressure maps precisely localize the contact centroids, ensuring the stable discrimination of closely spaced adjacent keys. This super-resolved localization seamlessly supports real-time typing and calculator applications without relying on discrete physical buttons. Furthermore, when integrated onto a robotic hand, the sensing system instantly translates real-world physical stimuli into synchronized interactive reactions within the virtual space. This comprehensive demonstration perfectly highlights how algorithmically expanded tactile resolution can compress complex, multi-command interfaces into a minimal hardware footprint, profoundly empowering next-generation human-machine interactions<sup>[82]</sup>.

High-resolution tactile sensing also plays an increasingly important role in XR interaction. Modern controller-free XR interactions primarily rely on optical hand tracking to capture finger dynamics, but such approaches remain vulnerable to visual occlusion and often require substantial computational resources to maintain accuracy and low latency. High-resolution tactile interfaces can complement these vision-based approaches by providing an additional high-bandwidth physical input channel. [Figure 5D](#) demonstrates an array-free silk fibroin ionic touch screen (SFITS) that functions as a highly deformable, skin-like virtual reality (VR) interactive interface. Owing to their continuous capacitive sensing mechanism, SFITS can infer touch coordinates across a flexible surface using only peripheral electrodes, enabling spatially resolved touch information acquisition. Leveraging this capability, the authors implement a VR interaction framework in which handwritten inputs and touch gestures on SFITS are converted into digital commands, allowing users to access virtual protein libraries and manipulate three-dimensional models through corner-based control of rotation and scaling. In this way, spatially rich tactile input provides a complementary interaction modality for XR systems, enriching the interaction space and mitigating some of the limitations inherent to purely vision-based interfaces<sup>[89]</sup>.

## CONCLUSION AND OUTLOOK

This review systematically examines recent advances in high-resolution flexible tactile sensors, focusing on the fundamental strategies that enable enhanced spatial perception capability. We categorized the major implementation pathways into array-based spatial information sampling via discrete taxel layouts, and array-free spatial information inference over continuous sensing medium. By comparing their respective advantages and limitations in terms of spatial resolution, system complexity, scalability, and robustness, we highlighted how high-resolution tactile perception is no longer exclusively bound to physical layout densification. Instead, it is increasingly driven by intelligent signal processing and computational decoding. Finally, we introduce its broad spectrum of applications, spanning dexterous robotic manipulation, large-area environmental perception, human-machine interactive interfaces, and XR interaction, where high-resolution tactile sensing plays an indispensable role in interpreting complex contact stimuli, fundamentally elevating interaction veracity, stability, and adaptability.

Despite these remarkable advances, significant gaps remain between current artificial flexible tactile systems and the biological skin at the spatial information richness, adaptability, and integration level. As conceptually illustrated in [Figure 6](#), several pivotal challenges and emerging opportunities merit further exploration to propel the field toward human-level embodied perception.

### I. Scalability: Large-Area High-Resolution Tactile Perception

Currently, high-resolution tactile sensing technologies have demonstrated exceptional perceptual fidelity within localized interactive regions, such as robotic fingertips or small grippers. Achieving high spatial resolution over expansive areas without incurring abundant overheads in wiring, readout complexity, power consumption, and data processing remains a critical challenge. Future breakthroughs will likely converge on how to simplify signal acquisition at the physical level via ingenious structural designs and mechanism discoveries. Concurrently, by coupling these with more efficient inference algorithms, systems will be able to stably decode high-resolution and large-area spatial tactile information from a limited number of hardware measurement channels.

### II. Generalization: Robust Perception Across Varying Geometries and Contact States

Most current high-resolution realization frameworks are developed and validated under controlled contact conditions or pre-defined surface configurations. However, practical deployment requires stable tactile perception on dynamic surfaces and under varying contact states. In these unstructured scenarios, severe mechanical deformations, geometric nonlinearities of the medium, and the resulting sensor data domain

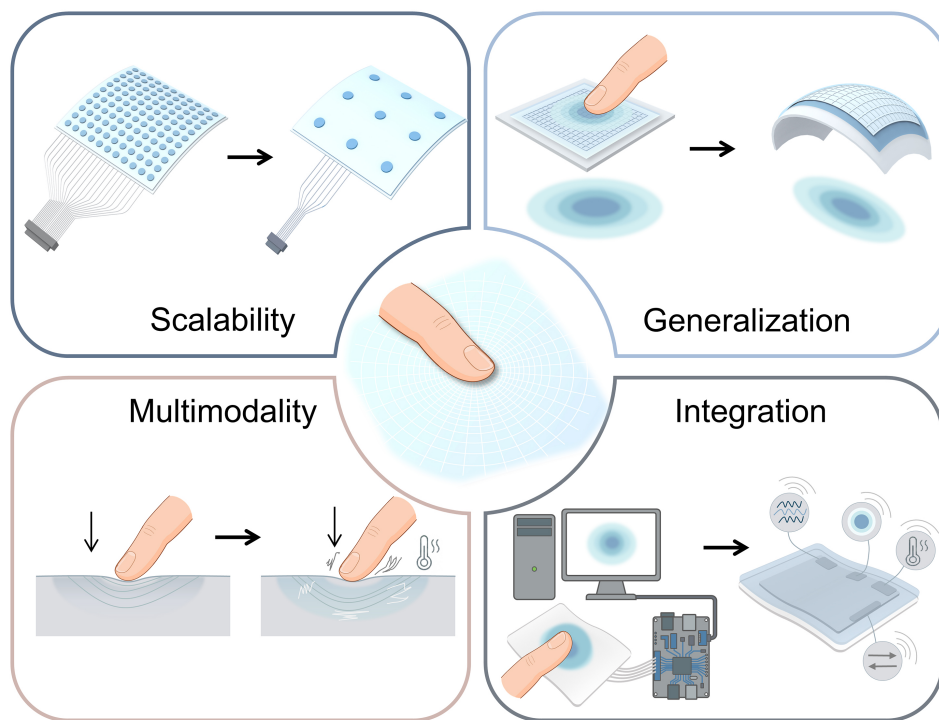


**Figure 6.** Future perspectives for high-resolution flexible tactile sensors.

shifts can drastically degrade the performance of existing flexible tactile systems. Advancing this field may require the co-design of adaptable sensing architectures and physics-informed learning algorithms capable of embedding prior contact mechanics and material constitutive relations into the inference process, maintaining robust and consistent spatial perception across diverse geometric shapes and unpredictable interactive scenarios.

### III. Multimodality: Sensing and Decoupling of Heterogeneous Tactile Stimuli

Human skin possesses the innate ability to simultaneously perceive normal pressure, shear forces, different frequency vibrations, and temperature variations without confounding the signals. In contrast, most current high-resolution tactile sensing systems remain restricted to single-modal, primarily normal pressure. When exposed to complex physical interactions in real world, they frequently suffer from severe multi-physical signals coupling. Decoupling heterogeneous tactile stimuli and capturing nonlinear physical behaviors remain open challenges. Recent studies have explored special-design strategies such as magnetic field encoded force decoupling<sup>[79]</sup>, bioinspired 3D structural decoupling<sup>[81]</sup>, overlapped receptive-field and attention-based algorithmic multi-site decoding<sup>[82]</sup>, and optical deformation-field-based multimodal encoding<sup>[97]</sup>. Future efforts may focus on materials science and structural engineering combined with backend algorithms to further develop multimodal tactile sensing systems with intrinsically decoupled and high-resolution responses.

### IV. Integration: Toward Compact and Intelligent Tactile Systems

In prevailing implementations, sensing layers, data acquisition modules, and signal processing units remain physically separated, resulting in bulky and power-intensive systems. Moving toward compact and integrated platforms with in-sensor intelligence represents a promising direction. Embedding signal conditioning and AI algorithms directly into the flexible tactile sensing systems could significantly reduce transmission latency and system complexity while enhancing real-time responsiveness. Such integration will be crucial for future embodied interaction applications.

Overall, advancing high-resolution flexible tactile sensors will require coordinated progress across materials engineering, structural design, signal processing, and intelligent algorithms. By bridging hardware innovation with algorithmic intelligence, next-generation tactile systems may approach the information richness, contact adaptability, and functional integration of biological skin, unlocking new possibilities in robotics, healthcare, and immersive human-machine interaction.

## DECLARATIONS

### Authors' contributions

Made substantial contributions to the conception, design, theoretical framework and writing of the review: Shen, Z.; Wu, H.

Provided support in manuscript revision and figure preparation: Hou, Y.

Provided administrative, technical, and material support: Yang, H.; Yang, G.; Xu, K.

### Availability of data and materials

Not applicable.

### AI and AI-assisted tools statement

Not applicable.

### Financial support and sponsorship

This work was supported by the National Natural Science Foundation of China (U25A20321, 52475610), and the Zhejiang Provincial Natural Science Foundation of China (LR26E050002).

### Conflict of interest

All authors declared that there are no conflicts of interest.

### Ethical approval and consent to participate

Not applicable.

### Consent for publication

Not applicable.

### Copyright

© The Author(s) 2026.

## REFERENCES

1. Wang, R.; Hu, S.; Zhu, W.; et al. Recent progress in high-resolution tactile sensor array: from sensor fabrication to advanced applications. *Prog. Nat. Sci. Mater. Int.* **2023**, *33*, 55-66. DOI
2. Ha, K. H.; Yoo, J.; Li, S.; et al. Full freedom-of-motion actuators as advanced haptic interfaces. *Science* **2025**, *387*, 1383-90. DOI PubMed
3. Yu, X.; Xie, Z.; Yu, Y.; et al. Skin-integrated wireless haptic interfaces for virtual and augmented reality. *Nature* **2019**, *575*, 473-9. DOI PubMed
4. Wan, Z.; Liu, P.; Fu, Y.; et al. Flexible tactile sensors: materials, mechanisms, structures, and multifaceted applications. *Small* **2025**, *21*, e11475. DOI PubMed
5. Liu, Y.; Yiu, C.; Song, Z.; et al. Electronic skin as wireless human-machine interfaces for robotic VR. *Sci. Adv.* **2022**, *8*, eabl6700. DOI PubMed PMC
6. Yin, J.; Hinchet, R.; Shea, H.; Majidi, C. Wearable soft technologies for haptic sensing and feedback. *Adv. Funct. Mater.* **2021**, *31*, 2007428. DOI
7. Zhang, N.; Ren, J.; Dong, Y.; et al. Soft robotic hand with tactile palm-finger coordination. *Nat. Commun.* **2025**, *16*, 2395. DOI PubMed PMC
8. Wei, D.; Guo, J.; Qiu, Y.; et al. Monitoring the delicate operations of surgical robots via ultra-sensitive ionic electronic skin. *Natl. Sci. Rev.* **2022**, *9*, nwac227. DOI PubMed PMC

9. Guo, X.; Sun, Z.; Zhu, Y.; Lee, C. Zero-biased bionic fingertip e-skin with multimodal tactile perception and artificial intelligence for augmented touch awareness. *Adv. Mater.* **2024**, *36*, e2406778. [DOI PubMed](#)
10. Lu, Y.; Kong, D.; Yang, G.; et al. Machine learning-enabled tactile sensor design for dynamic touch decoding. *Adv. Sci.* **2023**, *10*, e2303949. [DOI PubMed PMC](#)
11. Ming, X.; Sheng, Y.; Yao, L.; et al. Anti-swelling conductive polyampholyte hydrogels via ionic complexations for underwater motion sensors and dynamic information storage. *Chem. Eng. J.* **2023**, *463*, 142439. [DOI](#)
12. Zhou, J.; Long, X.; Huang, J.; et al. Multiscale and hierarchical wrinkle enhanced graphene/Ecoflex sensors integrated with human-machine interfaces and cloud-platform. *Npj. Flex. Electron.* **2022**, *6*, 55. [DOI PubMed PMC](#)
13. Wang, P.; Ma, X.; Lin, Z.; et al. Well-defined in-textile photolithography towards permeable textile electronics. *Nat. Commun.* **2024**, *15*, 887. [DOI PubMed PMC](#)
14. Jin, Y.; Xue, S.; He, Y. Flexible pressure sensors enhanced by 3D-printed microstructures. *Adv. Mater.* **2025**, *37*, e2500076. [DOI PubMed](#)
15. Lu, Y.; Yang, G.; Wang, S.; et al. Stretchable graphene–hydrogel interfaces for wearable and implantable bioelectronics. *Nat. Electron.* **2024**, *7*, 51-65. [DOI](#)
16. Ra, Y.; La, M.; Cho, S.; Park, S. J.; Choi, D. Scalable batch fabrication of flexible, transparent and self-triggered tactile sensor array based on triboelectric effect. *Int. J. Precis. Eng. Manuf. Green. Technol.* **2021**, *8*, 519-31. [DOI](#)
17. He, X.; Zhang, B.; Liu, Q.; et al. Highly conductive and stretchable nanostructured ionogels for 3D printing capacitive sensors with superior performance. *Nat. Commun.* **2024**, *15*, 6431. [DOI PubMed PMC](#)
18. Xu, L.; Zhao, X.; Xun, X.; et al. Omnidirectionally strain-unperturbed tactile array from modulus regulation in quasi-homogeneous elastomer meshes. *Adv. Funct. Mater.* **2024**, *34*, 2307475. [DOI](#)
19. Su, Q.; Zou, Q.; Li, Y.; et al. A stretchable and strain-unperturbed pressure sensor for motion interference-free tactile monitoring on skins. *Sci. Adv.* **2021**, *7*, eabi4563. [DOI PubMed PMC](#)
20. Kim, T.; Shin, Y.; Kang, K.; et al. Ultrathin crystalline-silicon-based strain gauges with deep learning algorithms for silent speech interfaces. *Nat. Commun.* **2022**, *13*, 5815. [DOI PubMed PMC](#)
21. Gu, J.; Jung, Y.; Ahn, J.; et al. Auxetic kirigami structure-based self-powered strain sensor with customizable performance using machine learning. *Nano. Energy.* **2024**, *130*, 110124. [DOI](#)
22. Xu, C.; Wang, Y.; Zhang, J.; et al. Three-dimensional micro strain gauges as flexible, modular tactile sensors for versatile integration with micro- and macroelectronics. *Sci. Adv.* **2024**, *10*, eadp6094. [DOI PubMed PMC](#)
23. Lee, J. P.; Jang, H.; Jang, Y.; et al. Encoding of multi-modal emotional information via personalized skin-integrated wireless facial interface. *Nat. Commun.* **2024**, *15*, 530. [DOI PubMed PMC](#)
24. Li, G.; Liu, S.; Wang, L.; Zhu, R. Skin-inspired quadruple tactile sensors integrated on a robot hand enable object recognition. *Sci. Robot.* **2020**, *5*, eabc8134. [DOI PubMed](#)
25. Cui, S.; Han, D.; Chen, G.; et al. Toward stretchable flexible integrated sensor systems. *ACS. Appl. Mater. Interfaces.* **2025**, *17*, 11397-414. [DOI PubMed](#)
26. Li, S.; Wu, T.; Xu, J.; et al. Biomimetic multimodal tactile sensing enables human-like robotic perception. *Nat. Sens.* **2026**, *1*, 52-62. [DOI](#)
27. Luo, Y.; Liu, C.; Lee, Y. J.; et al. Adaptive tactile interaction transfer via digitally embroidered smart gloves. *Nat. Commun.* **2024**, *15*, 868. [DOI PubMed PMC](#)
28. Gao, W.; Lu, Z.; Feng, S.; et al. 3D printable dual-sensing hydrogels with exceptional anti-swelling and toughness. *Int. J. Extrem. Manuf.* **2026**, *8*, 025002. [DOI](#)
29. Liu, T.; Gou, G. Y.; Gao, F.; et al. Multichannel flexible pulse perception array for intelligent disease diagnosis system. *ACS. Nano.* **2023**, *17*, 5673-85. [DOI PubMed PMC](#)
30. Yao, Z.; Wu, W.; Gao, F.; et al. Flexible tactile sensing systems: challenges in theoretical research transferring to practical applications. *Nanomicro. Lett.* **2025**, *18*, 37. [DOI PubMed PMC](#)
31. Xu, S.; Xu, Z.; Li, D.; et al. Recent advances in flexible piezoresistive arrays: materials, design, and applications. *Polymers* **2023**, *15*, 2699. [DOI PubMed PMC](#)
32. Zhu, J.; Zhou, C.; Zhang, M. Recent progress in flexible tactile sensor systems: from design to application. *Soft. Sci.* **2021**, *1*, 3. [DOI](#)
33. Li, Z.; Shi, J.; Chen, X.; et al. Bimodal iontronic skins powered by edge intelligence for real-time collaborative interaction. *Natl. Sci. Rev.* **2026**, *13*, nwag111. [DOI PubMed PMC](#)
34. Becker, C.; Bao, B.; Karnaushenko, D. D.; et al. A new dimension for magnetosensitive e-skins: active matrix integrated micro-origami sensor arrays. *Nat. Commun.* **2022**, *13*, 2121. [DOI PubMed PMC](#)
35. Ji, J.; Zhao, W.; Wang, Y.; Li, Q.; Wang, G. Templated laser-induced-graphene-based tactile sensors enable wearable health monitoring and texture recognition via deep neural network. *ACS. Nano.* **2023**, *17*, 20153-66. [DOI PubMed](#)

36. Wang, E.; Sun, M.; Ge, D. A.; et al. Continuum tactile sensing via an amplified liquid metal interface. *Sci. Adv.* **2026**, *12*, eaec3673. DOI PubMed PMC
37. Qiao, K.; Feng, X.; Dong, L.; et al. Ultraflexible photoelectrical impedance tomography-based imager for 3-axis robotic tactile sensing. *Nat. Commun.* **2026**, *17*, 3928. DOI PubMed PMC
38. Son, C.; Kim, J.; Kang, D.; et al. Behavioral biometric optical tactile sensor for instantaneous decoupling of dynamic touch signals in real time. *Nat. Commun.* **2024**, *15*, 8003. DOI PubMed PMC
39. Bae, K.; Jeong, J.; Choi, J.; Pyo, S.; Kim, J. Large-area, crosstalk-free, flexible tactile sensor matrix pixelated by mesh layers. *ACS. Appl. Mater. Interfaces.* **2021**, *13*, 12259-67. DOI PubMed
40. Yu, H.; Guo, H.; Wang, J.; et al. Skin-inspired capacitive flexible tactile sensor with an asymmetric structure for detecting directional shear forces. *Adv. Sci.* **2024**, *11*, e2305883. DOI PubMed PMC
41. Zhang, J.; Yao, H.; Mo, J.; et al. Finger-inspired rigid-soft hybrid tactile sensor with superior sensitivity at high frequency. *Nat. Commun.* **2022**, *13*, 5076. DOI PubMed PMC
42. Yan, Z.; Wang, L.; Xia, Y.; et al. Flexible high-resolution triboelectric sensor array based on patterned laser-induced graphene for self-powered real-time tactile sensing. *Adv. Funct. Mater.* **2021**, *31*, 2100709. DOI
43. Gao, S.; Li, H.; Li, N.; et al. Additive-manufacturing-based flexible tactile sensors. *Adv. Funct. Mater.* **2026**, *36*, e32112. DOI
44. Wang, Z.; Tang, Y.; Yao, P.; et al. Bioinspired flexible tactile sensors for smart soft robotics. *ACS. Appl. Mater. Interfaces.* **2026**, *18*, 4568-89. DOI PubMed
45. Wen, J.; Li, B.; Ren, L.; Wang, K.; Cao, Y.; Ren, L. Biomimetic additive manufacturing tactile sensing systems: mechanisms, materials, techniques, and prospects. *Mater. Today.* **2026**, *92*, 711-50. DOI
46. He, S.; Zhou, Y.; Sun, S.; et al. Sub-milliscale-resolution bimodal tactile sensor array with human-skin-like graphesthesia sensation. *Adv. Mater.* **2026**, *38*, e19734. DOI PubMed
47. Ouyang, Q.; Yao, C.; Chen, H.; et al. Machine learning-coupled tactile recognition with high spatiotemporal resolution based on cross-striped nanocarbon piezoresistive sensor array. *Biosens. Bioelectron.* **2024**, *246*, 115873. DOI PubMed
48. Ni, J.; Richter, A.; Gerlach, G.; Vorrath, E. M. A low-cost and environment-tolerant stretchable matrix tactile switch sensor array. *Measurement* **2026**, *262*, 120108. DOI
49. Sundaram, S.; Kellnhofer, P.; Li, Y.; Zhu, J. Y.; Torralba, A.; Matusik, W. Learning the signatures of the human grasp using a scalable tactile glove. *Nature* **2019**, *569*, 698-702. DOI PubMed
50. Lin, W.; Wang, B.; Peng, G.; Shan, Y.; Hu, H.; Yang, Z. Skin-inspired piezoelectric tactile sensor array with crosstalk-free row+column electrodes for spatiotemporally distinguishing diverse stimuli. *Adv. Sci.* **2021**, *8*, 2002817. DOI PubMed PMC
51. Wang, L.; Peng, H.; Wang, X.; et al. PDMS/MWCNT-based tactile sensor array with coplanar electrodes for crosstalk suppression. *Microsyst. Nanoeng.* **2016**, *2*, 16065. DOI PubMed PMC
52. Wu, J.; Wang, L.; Li, J. General voltage feedback circuit model in the two-dimensional networked resistive sensor array. *J. Sens.* **2015**, *2015*, 1-8. DOI
53. Warnakulasuriya, A. S.; Dinushka, N. Y.; Dias, A. A. C.; et al. A readout circuit based on zero potential crosstalk suppression for a large piezoresistive sensor array: case study based on a resistor model. *IEEE. Sens. J.* **2021**, *21*, 16770-9. DOI
54. Shu, L.; Tao, X.; Feng, D. D. A new approach for readout of resistive sensor arrays for wearable electronic applications. *IEEE. Sens. J.* **2015**, *15*, 442-52. DOI
55. Zhang, L.; Gao, Z.; Lei, H.; et al. Strain-insensitive stretchable triboelectric tactile sensors via interfacial stress dispersion. *Nano. Energy.* **2025**, *133*, 110482. DOI
56. Berman, A.; Shi, B.; Zaluska, T.; et al. A skin-inspired, capacitive array for tactile modulus detection via a scalable rigid-island architecture. *npj. Flex. Electron.* **2026**, *10*, 503. DOI
57. Shao, R.; Wang, C.; Zhao, J.; Yang, H.; Sun, S. Crosstalk-free, stretching-insensitive sensor based on arch-bridge architecture for tactile mapping with parallel addressing strategy toward million-scale-pixels processing. *Adv. Sci.* **2021**, *8*, e2101876. DOI PubMed PMC
58. Li, Y.; Long, J.; Chen, Y.; Huang, Y.; Zhao, N. Crosstalk-free, high-resolution pressure sensor arrays enabled by high-throughput laser manufacturing. *Adv. Mater.* **2022**, *34*, e2200517. DOI PubMed
59. Mei, S.; Yi, H.; Zhao, J.; et al. High-density, highly sensitive sensor array of spiky carbon nanospheres for strain field mapping. *Nat. Commun.* **2024**, *15*, 3752. DOI PubMed PMC
60. Li, Z.; Xu, H.; Zheng, Y.; et al. A reconfigurable heterostructure transistor array for monocular 3D parallax reconstruction. *Nat. Electron.* **2025**, *8*, 46-55. DOI
61. Zhong, B.; Qin, X.; Xu, H.; et al. Monolithic cell-on-memristor architecture enables wafer-scale integration of oscillatory chemoreceptors for bio-realistic gustatory chips. *Nat. Mater.* **2026**, *25*, 275-84. DOI PubMed
62. Takei, K.; Takahashi, T.; Ho, J. C.; et al. Nanowire active-matrix circuitry for low-voltage macroscale artificial skin. *Nat. Mater.* **2010**, *9*, 821-6. DOI PubMed

- 
63. Baek, S.; Lee, Y.; Baek, J.; et al. Spatiotemporal measurement of arterial pulse waves enabled by wearable active-matrix pressure sensor arrays. *ACS. Nano.* **2022**, *16*, 368-77. [DOI PubMed](#)
  64. Oh, H.; Yi, G. C.; Yip, M.; Dayeh, S. A. Scalable tactile sensor arrays on flexible substrates with high spatiotemporal resolution enabling slip and grip for closed-loop robotics. *Sci. Adv.* **2020**, *6*, eabd7795. [DOI PubMed PMC](#)
  65. Zheng, Y.; Xu, H.; Xu, H.; et al. Twelve-inch electrically anisotropic boridene for optoelectronic computing. *Nat. Nanotechnol.* **2026**, *21*, 571-8. [DOI PubMed](#)
  66. Zhao, Z.; Tang, J.; Yuan, J.; et al. Large-scale integrated flexible tactile sensor array for sensitive smart robotic touch. *ACS. Nano.* **2022**, *16*, 16784-95. [DOI PubMed](#)
  67. Jo, Y.; Lee, Y.; Kwon, J.; et al. 3D active-matrix multimodal sensor arrays for independent detection of pressure and temperature. *Sci. Adv.* **2025**, *11*, eads4516. [DOI PubMed PMC](#)
  68. Nie, Q.; Wang, F.; Yang, F. S.; et al. Intelligent tactile perception revolution: innovations in flexible FET-based tactile sensors for next-gen human-machine interfaces. *Adv. Mater.* **2026**, *38*, e10646. [DOI PubMed](#)
  69. Zimmerman, A.; Bai, L.; Ginty, D. D. The gentle touch receptors of mammalian skin. *Science* **2014**, *346*, 950-4. [DOI PubMed PMC](#)
  70. Handler, A.; Ginty, D. D. The mechanosensory neurons of touch and their mechanisms of activation. *Nat. Rev. Neurosci.* **2021**, *22*, 521-37. [DOI PubMed PMC](#)
  71. Xu, Q.; Yang, Z.; Wang, Z.; et al. Sandwich Miura-Ori enabled large area, super resolution tactile skin for human-machine interactions. *Adv. Sci.* **2025**, *12*, e2414580. [DOI PubMed PMC](#)
  72. Hu, H.; Zhang, C.; Lai, X.; et al. Large-area magnetic skin for multi-point and multi-scale tactile sensing with super-resolution. *npj. Flex. Electron.* **2024**, *8*, 325. [DOI](#)
  73. Hu, H.; Zhang, C.; Pan, C.; et al. Wireless flexible magnetic tactile sensor with super-resolution in large-areas. *ACS. Nano.* **2022**, *16*, 19271-80. [DOI PubMed](#)
  74. Kim, K. K.; Ha, I.; Kim, M.; et al. A deep-learned skin sensor decoding the epicentral human motions. *Nat. Commun.* **2020**, *11*, 2149. [DOI PubMed PMC](#)
  75. Pyun, K. R.; Kwon, K.; Yoo, M. J.; et al. Machine-learned wearable sensors for real-time hand-motion recognition: toward practical applications. *Natl. Sci. Rev.* **2024**, *11*, nwad298. [DOI PubMed PMC](#)
  76. Hu, X.; Liu, Z.; Zhang, Y. Three-dimensionally architected tactile electronic skins. *ACS. Nano.* **2025**, *19*, 14523-39. [DOI PubMed](#)
  77. Sun, H.; Martius, G. Machine learning for haptics: inferring multi-contact stimulation from sparse sensor configuration. *Front. Neurobot.* **2019**, *13*, 51. [DOI PubMed PMC](#)
  78. Lu, Z.; Su, Y.; Ye, Q.; et al. A low-cost super-resolution tactile sensor: design, fabrication, and validation. *IEEE. Sens. J.* **2024**, *24*, 36518-29. [DOI](#)
  79. Yan, Y.; Hu, Z.; Yang, Z.; et al. Soft magnetic skin for super-resolution tactile sensing with force self-decoupling. *Sci. Robot.* **2021**, *6*, eabc8801. [DOI PubMed](#)
  80. Sun, H.; Martius, G. Guiding the design of superresolution tactile skins with taxel value isolines theory. *Sci. Robot.* **2022**, *7*, eabm0608. [DOI PubMed](#)
  81. Liu, Z.; Hu, X.; Bo, R.; et al. A three-dimensionally architected electronic skin mimicking human mechanosensation. *Science* **2024**, *384*, 987-94. [DOI PubMed](#)
  82. Kong, D.; Lu, Y.; Zhou, S.; et al. Super-resolution tactile sensor arrays with sparse units enabled by deep learning. *Sci. Adv.* **2025**, *11*, eadv2124. [DOI PubMed PMC](#)
  83. Zhao, Z.; Li, W.; Li, Y.; et al. Embedding high-resolution touch across robotic hands enables adaptive human-like grasping. *Nat. Mach. Intell.* **2025**, *7*, 889-900. [DOI](#)
  84. Kim, C. C.; Lee, H. H.; Oh, K. H.; Sun, J. Y. Highly stretchable, transparent ionic touch panel. *Science* **2016**, *353*, 682-7. [DOI PubMed](#)
  85. Chen, H.; Yang, X.; Wang, P.; Geng, J.; Ma, G.; Wang, X. A large-area flexible tactile sensor for multi-touch and force detection using electrical impedance tomography. *IEEE. Sens. J.* **2022**, *22*, 7119-29. [DOI](#)
  86. Costa Cornellà, A.; Hardman, D.; Costi, L.; Brancart, J.; Van Assche, G.; Iida, F. Variable sensitivity multimaterial robotic e-skin combining electronic and ionic conductivity using electrical impedance tomography. *Sci. Rep.* **2023**, *13*, 20004. [DOI PubMed PMC](#)
  87. Zhang, Y.; Ye, J.; Lin, Z.; Huang, S.; Wang, H.; Wu, H. A piezoresistive tactile sensor for a large area employing neural network. *Sensors* **2018**, *19*, 27. [DOI PubMed PMC](#)
  88. Kim, K.; Hong, J. H.; Bae, K.; et al. Extremely durable electrical impedance tomography-based soft and ultrathin wearable e-skin for three-dimensional tactile interfaces. *Sci. Adv.* **2024**, *10*, eadr1099. [DOI PubMed PMC](#)
  89. Ye, C.; Zhang, H.; Yang, Y.; et al. Sustainable silk fibroin ionic touch screens for flexible biodegradable electronics with integrated AI and IoT functionality. *Adv. Mater.* **2025**, *37*, e2412972. [DOI PubMed](#)
  90. Lee, Y.; Lim, S.; Song, W. J.; et al. Triboreistive touch sensing: grid-free touch-point recognition based on monolayered ionic power generators. *Adv. Mater.* **2022**, *34*, e2108586. [DOI PubMed](#)

91. Huang, Z.; Yu, S.; Xu, Y.; et al. In-sensor tactile fusion and logic for accurate intention recognition. *Adv. Mater.* **2024**, *36*, e2407329. [DOI](#) [PubMed](#)
92. Sun, H.; Kuchenbecker, K. J.; Martius, G. A soft thumb-sized vision-based sensor with accurate all-round force perception. *Nat. Mach. Intell.* **2022**, *4*, 135-45. [DOI](#)
93. Park, H.; Park, K.; Mo, S.; Kim, J. Deep neural network based electrical impedance tomographic sensing methodology for large-area robotic tactile sensing. *IEEE. Trans. Robot.* **2021**, *37*, 1570-83. [DOI](#)
94. Park, H.; Kim, W.; Jeon, S.; Na, Y.; Kim, J. Graph-structured super-resolution for geometry- generalized tomographic tactile sensing: application to humanoid faces. *IEEE. Trans. Robot.* **2025**, *41*, 558-72. [DOI](#)
95. Kong, D.; Yang, G.; Pang, G.; et al. Bioinspired co-design of tactile sensor and deep learning algorithm for human-robot interaction. *Adv. Intell. Syst.* **2022**, *4*, 2200050. [DOI](#)
96. Lee, H.; Sun, H.; Park, H.; et al. Predicting the force map of an ERT-based tactile sensor using simulation and deep networks. *IEEE. Trans. Autom. Sci. Eng.* **2023**, *20*, 425-39. [DOI](#)
97. Wang, Y.; Guo, H.; Wu, H.; Dong, H. Flexible robotic hand harnesses large deformations for full-coverage human-like multimodal haptic perception. *Nat. Commun.* **2025**, *17*, 458. [DOI](#) [PubMed](#) [PMC](#)
98. Li, X.; Wu, Z.; Chen, Z.; Shi, J. From touching to seeing: visualized pressure sensing in electronic skins. *Soft. Sci.* **2025**, *5*, 16. [DOI](#)
99. Guo, Y.; Li, H.; Li, Y.; et al. Wearable hybrid device capable of interactive perception with pressure sensing and visualization. *Adv. Funct. Mater.* **2022**, *32*, 2203585. [DOI](#)
100. Duan, X.; Taurand, S.; Soleimani, M. Artificial skin through super-sensing method and electrical impedance data from conductive fabric with aid of deep learning. *Sci. Rep.* **2019**, *9*, 8831. [DOI](#) [PubMed](#) [PMC](#)
101. Hardman, D.; Thuruthel, T. G.; Iida, F. Multimodal information structuring with single-layer soft skins and high-density electrical impedance tomography. *Sci. Robot.* **2025**, *10*, eadq2303. [DOI](#) [PubMed](#)
102. Jing, X.; Qian, K. Reducing cross-sensor domain gaps in tactile sensing via few-sample-driven style-to-content unsupervised domain adaptation. *Sensors* **2025**, *25*, 256. [DOI](#) [PubMed](#) [PMC](#)
103. Kim, D.; Kwon, J.; Jeon, B.; Park, Y. Adaptive calibration of soft sensors using optimal transportation transfer learning for mass production and long-term usage. *Adv. Intell. Syst.* **2020**, *2*, 1900178. [DOI](#)
104. Cao, G.; Jiang, J.; Bollegala, D.; Li, M.; Luo, S. Multimodal zero-shot learning for tactile texture recognition. *Robot. Auton. Syst.* **2024**, *176*, 104688. [DOI](#)
105. Ji, J.; Liu, Y.; Ma, H. Model-based 3D contact geometry perception for visual tactile sensor. *Sensors* **2022**, *22*, 6470. [DOI](#) [PubMed](#) [PMC](#)
106. Makushko, P.; Ge, J.; Cañón Bermúdez, G. S.; et al. Scalable magnetoreceptive e-skin for energy-efficient high-resolution interaction towards undisturbed extended reality. *Nat. Commun.* **2025**, *16*, 1647. [DOI](#) [PubMed](#) [PMC](#)
107. Karniadakis, G. E.; Kevrekidis, I. G.; Lu, L.; Perdikaris, P.; Wang, S.; Yang, L. Physics-informed machine learning. *Nat. Rev. Phys.* **2021**, *3*, 422-40. [DOI](#)
108. Zhang, Y.; Xiang, S.; Wang, Z.; et al. TDACNN: target-domain-free domain adaptation convolutional neural network for drift compensation in gas sensors. *Sens. Actuators. B. Chem.* **2022**, *361*, 131739. [DOI](#)
109. Boutry, C. M.; Negre, M.; Jorda, M.; et al. A hierarchically patterned, bioinspired e-skin able to detect the direction of applied pressure for robotics. *Sci. Robot.* **2018**, *3*, eaau6914. [DOI](#) [PubMed](#)
110. Xu, C.; Solomon, S. A.; Gao, W. Artificial intelligence-powered electronic skin. *Nat. Mach. Intell.* **2023**, *5*, 1344-55. [DOI](#) [PubMed](#) [PMC](#)
111. Bai, N.; Xue, Y.; Chen, S.; et al. A robotic sensory system with high spatiotemporal resolution for texture recognition. *Nat. Commun.* **2023**, *14*, 7121. [DOI](#) [PubMed](#) [PMC](#)
112. Yao, H.; Yang, W.; Cheng, W.; et al. Near-hysteresis-free soft tactile electronic skins for wearables and reliable machine learning. *Proc. Natl. Acad. Sci. U. S. A.* **2020**, *117*, 25352-9. [DOI](#) [PubMed](#) [PMC](#)
113. Linghu, C.; Liu, Y.; Yang, X.; et al. Versatile adhesive skin enhances robotic interactions with the environment. *Sci. Adv.* **2025**, *11*, eadt4765. [DOI](#) [PubMed](#) [PMC](#)
114. Wen, F.; Sun, Z.; He, T.; et al. Machine learning glove using self-powered conductive superhydrophobic triboelectric textile for gesture recognition in VR/AR applications. *Adv. Sci.* **2020**, *7*, 2000261. [DOI](#) [PubMed](#) [PMC](#)
115. Pang, Y.; Xu, X.; Chen, S.; et al. Skin-inspired textile-based tactile sensors enable multifunctional sensing of wearables and soft robots. *Nano. Energy.* **2022**, *96*, 107137. [DOI](#)
116. Pyo, S.; Lee, J.; Kim, W.; Jo, E.; Kim, J. Multi-layered, hierarchical fabric-based tactile sensors with high sensitivity and linearity in ultrawide pressure range. *Adv. Funct. Mater.* **2019**, *29*, 1902484. [DOI](#)
117. Hu, Z.; Liang, T.; Wu, Y.; et al. Fabric topological haptic proxy for interactive virtual reality. *Natl. Sci. Rev.* **2026**, *13*, nwag041. [DOI](#) [PubMed](#) [PMC](#)
118. Hu, H.; Li, W.; Li, X.; et al. An ultra-sensitive flexible piezoelectric nanogenerator based on P(VDF-TrFE) nanofibers. *Int. J. Extrem. Manuf.* **2025**, *7*, 065503. [DOI](#)

- 
119. Huang, X.; Bu, T.; Zheng, Q.; et al. Flexible sensors with zero Poisson's ratio. *Natl. Sci. Rev.* **2024**, *11*, nwae027. [DOI PubMed PMC](#)
  120. Lee, H.; Park, K.; Kim, J.; Kuchenbecker, K. J. Piezoresistive textile layer and distributed electrode structure for soft whole-body tactile skin. *Smart. Mater. Struct.* **2021**, *30*, 085036. [DOI](#)
  121. Park, K.; Yuk, H.; Yang, M.; Cho, J.; Lee, H.; Kim, J. A biomimetic elastomeric robot skin using electrical impedance and acoustic tomography for tactile sensing. *Sci. Robot.* **2022**, *7*, eabm7187. [DOI PubMed](#)
  122. Bauza, M.; Bronars, A.; Hou, Y.; Taylor, I.; Chavan-Dafle, N.; Rodriguez, A. SimPLE, a visuotactile method learned in simulation to precisely pick, localize, regrasp, and place objects. *Sci. Robot.* **2024**, *9*, eadi8808. [DOI PubMed](#)
  123. Wu, X.; Xie, Y.; Wu, Z.; et al. A bio-inspired proximity-tactile sensor array with beyond-extreme detection depth for embodied intelligence. *Int. J. Extrem. Manuf.* **2026**, *8*, 035506. [DOI](#)
  124. Xu, J.; Li, X.; Chang, H.; et al. Electrooculography and tactile perception collaborative interface for 3D human-machine interaction. *ACS. Nano.* **2022**, *16*, 6687-99. [DOI PubMed](#)

**Disclaimer/Publisher's Note:** All statements, opinions, and data contained in this publication are solely those of the individual author(s) and contributor(s) and do not necessarily reflect those of OAE and/or the editor(s). OAE and/or the editor(s) disclaim any responsibility for harm to persons or property resulting from the use of any ideas, methods, instructions, or products mentioned in the content.



© The Author(s) 2026. Open Access This article is licensed under a Creative Commons Attribution 4.0 International License (<https://creativecommons.org/licenses/by/4.0/>), which permits unrestricted use, sharing, adaptation, distribution and reproduction in any medium or format, for any purpose, even commercially, as long as you give appropriate credit to the original author(s) and the source, provide a link to the Creative Commons license, and indicate if changes were made.